

**GEORGIA DOT RESEARCH PROJECT 12-17
FINAL REPORT**

**Comparative Analysis of Dynamic Pricing Strategies
for Managed Lanes**



**OFFICE OF RESEARCH
15 Kennedy Drive
Forest Park, GA 30297-2534**

1. Report No. FHWA-GA-15-1217		2. Government Accession No.		3. Recipient's Catalog No.	
4. Title and Subtitle Comparative Analysis of Dynamic Pricing Strategies for Managed Lanes			5. Report Date August, 2014		
			6. Performing Organization Code		
7. Author(s) Jorge A. Laval, Ph.D., Yafeng Yin, Ph.D., Yingyan Lou, Ph.D., and Hyun W. Cho			8. Performing Organization Report No. 12-17		
9. Performing Organization Name and Address School of Civil and Environmental Engineering Georgia Institute of Technology 790 Atlantic Dr. Atlanta, GA 30332-0355			10. Work Unit No. (TRAIS)		
			11. Contract or Grant No. 0011746		
12. Sponsoring Agency Name and Address Georgia Department of Transportation Office of Research 15 Kennedy Drive Forest Park, GA 30297-2534			13. Type of Report and Period Covered August 2012 – December 2014		
			14. Sponsoring Agency Code		
15. Supplementary Notes Prepared in cooperation with the Georgia Department of Transportation and the Southeastern Transportation Research, Innovation, Development and Education Center.					
16. Abstract The objective of this research was to investigate and compare the performances of different dynamic pricing strategies for managed lanes facilities. On a two-alternative network, analytical expressions for the assignment, revenue and total delay in each alternative were derived as a function of the pricing strategy. It was found that minimum total system delay was achieved with many different pricing strategies. This gave flexibility to operators to allocate congestion to either alternative according to their specific objective while maintaining the same minimum total system delay. Given a specific objective, the optimal pricing strategy was determined by finding a single parameter value in the case of high-occupancy toll (HOT) lanes. Performances of pricing strategies were compared by simulation experiments. Tolls with refund options and tradable credit scheme were discussed.					
17. Key Words High Occupancy Toll lanes, Dynamic Congestion Pricing			18. Distribution Statement		
19. Security Classif. (of report) Unclassified	20. Security Classif. (of this page) Unclassified	21. No. of pages 99		22. Price	

Form DOT F 1700.7 (8-72)

2014

STRIDE

Southeastern Transportation Research,
Innovation, Development and Education Center

Final Report

Comparative Analysis of Dynamic Pricing Strategies for Managed Lanes (2012-089S)



Jorge A. Laval, Ph.D., Georgia Institute of Technology

Yafeng Yin, Ph.D., University of Florida;

Yingyan Lou, Ph.D., Arizona State University

Hyun W. Cho, Georgia Institute of Technology

August 2014



TABLE OF CONTENTS

LIST OF TABLES	vi
LIST OF FIGURES	vi
EXECUTIVE SUMMARY	ix
CHAPTER 1 BACKGROUND	1
CHAPTER 2 RESEARCH APPROACH	4
Pricing Strategies for Toll Facilities	4
Dynamic Pricing for High-Occupancy/Toll Lanes with Refund Option	5
A Tradable Credit Scheme for Staggered Work Time.....	6
CHAPTER 3 CONGESTION PRICING STRATEGIES FOR TOLL FACILITIES.....	7
Motivation	7
Real-Time Pricing Based On Traffic Conditions on the Managed Lanes and/or General Purpose Lanes	10
Variable Bottleneck Capacity Linear Toll Pricing.....	27
Comparison to Fixed Toll Pricing.....	29
Comparative Analysis using Simulation.....	31
CHAPTER 4 DYNAMIC PRICING FOR HIGH-OCCUPANCY/TOLL LANES WITH REFUND OPTION.....	46
Introduction.....	46
Methodologies.....	47
Lane Choice Model.....	48
Traffic Model	50
Dynamic Pricing with Refund Option	50
Simulation and Preliminary Results.....	53
CHAPTER 5 A TRADABLE CREDIT SCHEME FOR STAGGERED WORK TIME	65
Introduction.....	65
Description of the Proposed Scheme	68

Modeling Framework.....	69
Numerical Example	80
CHAPTER 6 CONCLUSIONS AND RECOMMENDATIONS	84
REFERENCES	86

LIST OF TABLES

<u>Table</u>	<u>page</u>
3-1 Pricing strategies summary	25
3-2 O/D distribution of simulation	32
3-3 Comparing equation (30) and simulation results	35
3-4 Comparing equation (31) and simulation results	39
3-5 Performance comparison of pricing strategies' MoE	41

LIST OF FIGURES

<u>Figures</u>	<u>page</u>
3-1 (a) SR-91 Eastbound weekday toll rate (July 2014) (b) Average delay of SR-91 Eastbound weekday (July 2014)	9
3-2 Schematic representation of the network	10
3-3 System optimum input-output diagram	12
3-4 System optimum input-output diagram for users arriving at $t \geq t_0$	14
3-5 Evolution of the system (a) marginal cost, externality, travel time and (b) toll	18
3-6 Toll of maximum revenue	20
3-7 Input-output diagram for scenario of (a) maximum revenue under no constraints, (b) maximum revenue constrained, and (c) system; (d) and, (e) tolls corresponding to (a) and (b) numerical example	27
3-8 Input-output diagram of variable bottleneck capacity linear toll pricing strategy	28
3-9 Input-output diagram of Fixed Toll pricing strategy at 3 different levels ($\pi_a < \pi_b < \pi_c$)	30
3-10 Diagram of simulation model	32
3-11 Congestion formation of the traffic in the simulation model	32
3-12 Total delays of pricing strategies	34
3-13 Average of $\bar{\mu}_0, \bar{\mu}_1$ in CLT and VLT when bottleneck is active	35

3-14	Relations of W_j/W and a in (a) CLT and (b) VLT	36
3-15	Revenues of pricing strategies	37
3-16	Relations of R/W and π of the fixed toll pricing strategy	38
3-17	Relations of $R(a)/W$ and a in (a) CLT and (b) VLT	40
3-18	Fixed toll pricing strategy's ($\pi=0.06$ hr) (a) Input-output diagram for HOT lane; (b) GP lanes; (c) All lanes; (d) Oblique input-output diagram for HOT lane; (e) GP lanes; (f) All lanes	42
3-19	Constant bottleneck capacity Linear Toll Pricing Strategy's ($a=0.8$) (a) Input-output diagram for HOT lane; (b) GP lanes; (c) All lanes; (d) Oblique input-output diagram for HOT lane; (e) GP lanes; (f) All lanes	43
3-20	Variable bottleneck capacity Linear Toll Pricing Strategy's ($a=0.8$) (a) Input-output diagram for HOT lane; (b) GP lanes; (c) All lanes; (d) Oblique input-output diagram for HOT lane; (e) GP lanes; (f) All lanes	44
3-21	(a) Departure rates and (b) $\bar{\mu}_0, \bar{\mu}_1$ of the fixed toll pricing strategy's ($\pi=0.06$ hr); (c) Departure rates and (d) $\bar{\mu}_0, \bar{\mu}_1$ of the CLT's ($a=0.8$); (e) Departure rates and (f) $\bar{\mu}_0, \bar{\mu}_1$ of the VLT's ($a=0.8$)	45
4-1	Simulated HOT lane facility	55
4-2	Facility performance (Exp. 1, Run 1)	58
4-3	Toll rates (Exp. 1, Run 1).....	58
4-4	Facility performance (Exp. 1, Run 2)	61
4-5	Toll rates (Exp. 1, Run 2).....	62
4-6	Facility performance (Exp. 2, Run 3)	63
4-7	Toll rates (Exp. 2, Run 3).....	64
5-1	Departure pattern of employees before the implementation	72
5-2	Departure pattern of employees under the proposed scheme	74
5-3	Number of shifted employees in scenario 1 ($\theta_1=0.1$)	81
5-4	Number of shifted employees in scenario 2 ($\theta_1=0.04$)	81
5-5	Variation of credit price	82
5-6	Social benefit percentage change compared to existing condition	83
5-7	Relative change of total profit of firms.....	83

EXECUTIVE SUMMARY

The objective of this research was to investigate the performances of different dynamic pricing strategies for managed lanes facilities. These pricing strategies included real-time traffic responsive methods, refund options, and tradable credit schemes. In all cases, the research objective was to find the optimal configuration of each pricing strategy so that total system costs are minimized.

In the case of real-time pricing, we introduced the concept of linear pricing strategies, which is simple to apply in practice and turned out to exhibit extremely appealing mathematical properties. We found that minimum total system delay can be achieved in many different ways. This gives flexibility to operators to allocate congestion to either alternative according to their specific objective while maintaining the same minimum total system delay. Given a specific objective, the optimal pricing strategy can be determined by finding a single parameter value in the case of HOT lanes. For example, it was shown that among all the strategies that minimize total system delay, the one that maintains free-flow conditions on the managed lanes is the one that maximizes revenue.

Approaches to determining optimal operational parameters for a proposed managed lane pricing scheme with refund option were investigated. Deterministic utility functions were adopted for each individual traveler with an underlying value of time distribution across the population. A modified point queue model for traffic propagation was developed to account for the intrinsic randomness in traffic flow. An optimization model with a chance constraint was established to determine the desired inflow to the HOT lane during each tolling interval. The relationship among the optimal operational parameters (including the toll rate, the refund amount, the premium for the refund option, the travel time saving guaranteed by the operator) was discussed for two operational paradigms.

This research also proposed and analyzed a tradable credit scheme to alleviate the negative impact of staggered work schedules on firms. The results of a numerical example showed that the proposed scheme act as a relief for the productivity loss resulting from not having all employees at the desired work start times.

CHAPTER 1 BACKGROUND

In the U.S., a prevalent form of congestion pricing is managed lanes or express toll lanes, which is viewed as the first step toward more widespread pricing of congested roads. In a typical setting, lanes on a given freeway are designated either as general purpose or managed toll lanes. The former have no toll while the latter is only accessed by paying a toll. If high-occupancy vehicles do not need to pay, the lane is widely known as the high-occupancy/toll (HOT) lane. Since the first managed toll lane was implemented in 1995 on State Route 91 in Orange County, California, the concept has become quite popular and widely accepted by many transportation authorities. Currently, more than twenty managed-toll lanes are in operation, with more being constructed or planned in the country. To achieve their corresponding operational objectives, managed-lane operators often implement time-of-day or dynamic pricing. In the former, toll rate varies by time of day as per a pre-determined schedule. In the latter, the toll rate is adaptive to real-time traffic conditions.

In the research community, although there are a number of studies examining the performance of HOT lanes (see, e.g., Supernak et al. (2003, 2002a,b); Burriss and Stockton (2004); Zhang et al. (2009)) and travelers' willingness to pay (Li, 2001; Burriss and Appiah, 2004; Podgorski and Kockelman, 2006; Zmud et al., 2007; Finkleman et al., 2011), only a few studies are devoted to pricing strategies of managed lanes. Existing studies focused on ad-hoc objectives that the tolling agencies may seek to achieve, such as ensuring free-flow conditions on the HOT lane. For example, Li and Govind (2002) developed a toll evaluation model to assess the optimal pricing strategies of the HOT lane that can accomplish different objectives such as ensuring a minimum speed on the HOT lane, or in the general-purpose lanes (GPL), or maximizing toll

revenue. Zhang et al. (2008) used logit models to estimate dynamic toll rates after calculating the optimal flow ratios by using a feedback-based algorithm on the basis of keeping the HOT lane speed higher than 45mph. Yin and Lou (2009) explored two approaches including feedback and self-learning methods to determine dynamic pricing strategies for the HOT lane, and the comparative results showed that the self-learning controller is superior to the feedback controller in view of maintaining a free-flow traffic condition for managed lanes. Lou et al. (2011) further developed the self-learning approach in Yin and Lou (2009) to incorporate the effects of lane changing using the hybrid traffic flow model in Laval and Daganzo (2006). Yin et al. (2012) compared the pricing algorithm implemented on the 95 Express in south Florida with static and time-of-day tolls. The study suggested that when the demand pattern is predictable, time-of-day or even static tolling could perform as well as dynamic tolling, provided that the toll profiles are optimized for the demand pattern. Nonetheless, dynamic tolling performs in a more robust and stable manner due to its adaptive nature to demand fluctuations. Recognizing that dynamic tolling is beneficial but more costly to implement, the study further conducted a cost-benefit analysis to examine whether the benefits from dynamic tolling can justify its additional implementation cost or not.

It can be seen that quite a few pricing strategies have been implemented in practice or developed in the literature, but little has been done to compare these strategies and provide guidance on when a particular one should be implemented. Additionally, most of the existing methods are numerical instead of analytical, and therefore little insight was gained. To fill these voids, the project aimed to compare existing and novel pricing strategies to understand the pros and cons of each one.

OBJECTIVE

The objective of this research was to investigate the performances of different dynamic pricing strategies for managed lanes facilities. The focus was on the traffic dynamics resulting from each pricing strategy and the benefits and costs thereof. The problem was analyzed from three different perspectives: the users, the tolling authority (i.e., DOT) and the society, which led to three different performance measures.

CHAPTER 2 RESEARCH APPROACH

PRICING STRATEGIES FOR TOLL FACILITIES

A simplified system configuration was studied analytically while keeping traffic dynamics realistic. This simplified network consists of two parallel links with finite capacity and common origin and destination. While analytical results exist today for both user optimum (UO) and system optimum (SO) in the case of constant toll (Muñoz and Laval (2006)), this project generalized this methodology to account for time-dependent tolls as in the below strategies.

Time-of-day pricing

Under this scheme, a toll rate changes in time of day as per a pre-determined schedule. Typically, the hourly flows over a rolling horizon are examined to identify time periods when the facility is oversaturated, in which case the toll rate is set marginally higher. Conversely, the tolls for time periods where the flow is lower than a given threshold are marginally decreased.

Real-time pricing based on traffic conditions on the managed lanes and/or general purpose lanes

In this case, the toll rate is adaptive to real-time traffic conditions on the managed lanes and/or general purpose lanes. Our preliminary results suggested that depending on the optimization objective, this strategy might not be optimal in terms of total system benefits and could lead to unstable equilibrium patterns and excessive delays. In fact, an operator who is willing to guarantee free-flow travel time in the managed lanes may be forced to charge unreasonably high amounts to deter excess demand, which will worsen the conditions on the general purpose lanes and probably underutilize the managed lanes.

The strategies analyzed in the project were implemented numerically in order to obtain solutions for larger networks. This allowed us to conjecture the analytical insights against larger networks possibly containing multiple bottlenecks. Although each strategy required different numerical techniques for its resolution, traffic dynamics were given by the same model in all cases. We used *GTsim*, a simulation package that has been developed by Georgia Tech research team. *GTsim* includes the latest advancements in lane-changing models that are capable of explaining congestion dynamics.

All the strategies were implemented in each case and simulated under a typical rush hour demand pattern. For each strategy, the two different objectives considered here (from perspectives of the society and the tolling authority) were simulated independently. Also, the parameters defining each strategy were optimized separately for each objective; e.g., in the simplest example of a toll proportional to the delay in the managed lane, the coefficient of proportionality is optimized in each case. For comparing a large number of simulation results, we defined a suitable performance measure for each objective.

DYNAMIC PRICING FOR HIGH-OCCUPANCY/TOLL LANES WITH REFUND OPTION

While priced managed lanes provide an alternative travel choice for road users, travelers, in general, may have a negative attitude towards pricing. One plausible reason is that travelers may not receive the benefits they expected when choosing to pay to use managed lanes due to traffic uncertainties. This strategy was specifically proposed to address this issue. The idea was to offer a “price guarantee option” to a traveler when he or she chose to pay for managed lanes. Part of the toll paid by the traveler was refunded if the travel time saving had not reached the

minimal amount guaranteed. The goal of this pricing scheme was to achieve the operational objectives of managed lanes such as the desired level of service and sufficient revenue return that cover option claims, and at the same time enhance travelers' experiences with managed lanes and boost public acceptance of managed lanes pricing.

A TRADABLE CREDIT SCHEME FOR STAGGERED WORK TIME

A new tradable credit scheme was proposed to facilitate the implementation of staggered work schedules in firms. In the scheme, a government agency issued a certain number of mobility credits and charged one credit from any traveler who wishes to enter the central business district where the firms are located during the morning peak period. The mobility credits were directly allocated to the firms, who either distribute them to their employees or sell them to other firms. Employees without credits were shifted to a secondary work start time. The proposed scheme was analyzed in a simplified morning commute setting and travelers' equilibrium travel costs were derived using Vickrey's bottleneck model. To analyze the credit market equilibrium, the behavior of firms was characterized by the sensitivity of their productivity to their employees' work start time. Moreover, a problem of finding the optimum number of issued credits was formulated to maximize social benefit.

CHAPTER 3 CONGESTION PRICING STRATEGIES FOR TOLL FACILITIES

MOTIVATION

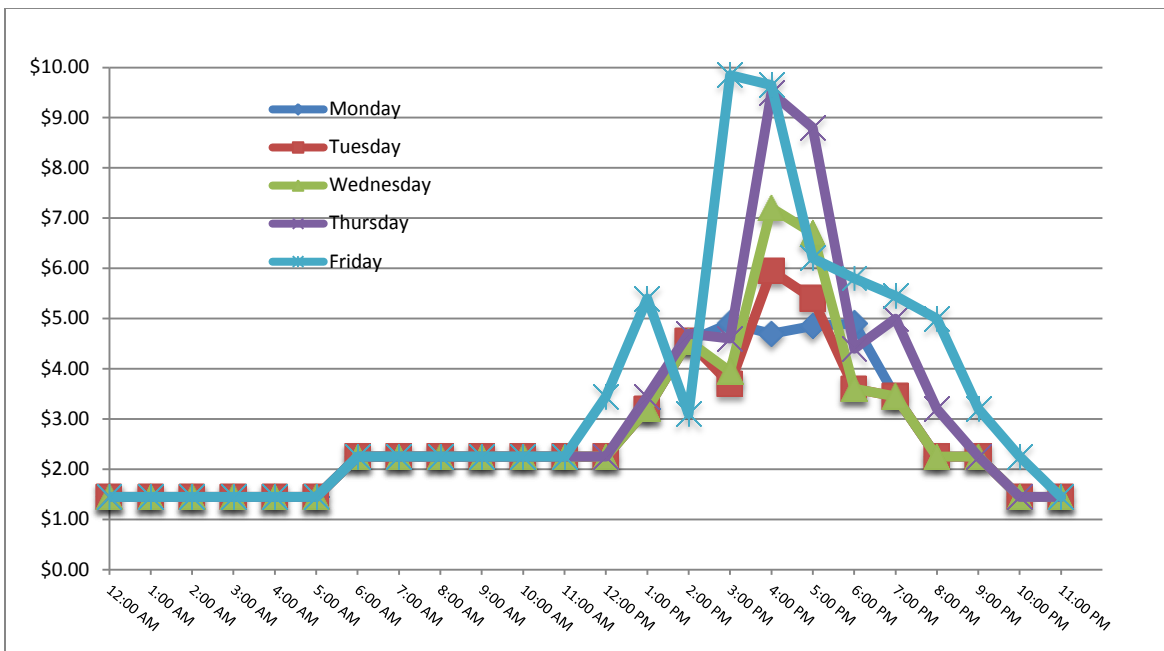
The SR-91 Express Lanes were opened on 1995 as the first toll road to apply dynamic congestion pricing in the U.S. It operates under a time-of-day pricing, where toll rates vary according to a predetermined time schedule. The purpose of designing the toll is to maintain SR-91 at free-flow speeds. To accomplish this goal, the toll authority monitors hourly traffic volumes and adjust the toll every six months if traffic volumes consistently exceed a threshold. Figure 3-1(a) depicts the weekday toll rate for eastbound traffic of SR-91 Express Lanes on July 2014.

Our preliminary study suggested that SR-91 Express Lanes' Time-of-day pricing strategy appears to be consistent with the theory in Muñoz and Laval (2006), where the marginal costs (expressed in units of time) of an alternative at a given time is equal to the remaining duration of congestion, which decreases linearly. In the theory, the System Optimum toll to each user is the difference between each alternative's externalities (marginal cost minus the delay experienced by the user).

From the California Department of Transportation's Performance Measurement System (PeMS) results, we found that SR-91 Express Lanes' toll rate was rather similar to the shape of delay that was experienced by users. PeMS Manual defines the delay as "the amount of extra time spent by all the vehicles beyond the time it takes to traverse a freeway segment at a threshold speed." The average delay of the weekday on July 2014 for the tolled section of SR-91(27~37 Milepost range) is shown in Figure 3-1(b).

Although PeMS does not specify the type of lanes for aggregated time series data, we inferred that the delay was experienced by general purpose lane users considering the purpose of the toll, which is to maintain SR-91 Express Lanes traffic flow at free-flow speeds. Comparing Figure 3-1(a) and(b), it is clear that the time range and peak amplitude of both graphs are similar, we concluded that the toll is also the consequence of the traffic conditions on the managed lane and/or general purpose lanes, which are explained in the next section.

(a) SR-91E Toll Rate



(b) Delay ($V_{\text{threshold}} = 60\text{mph}$)

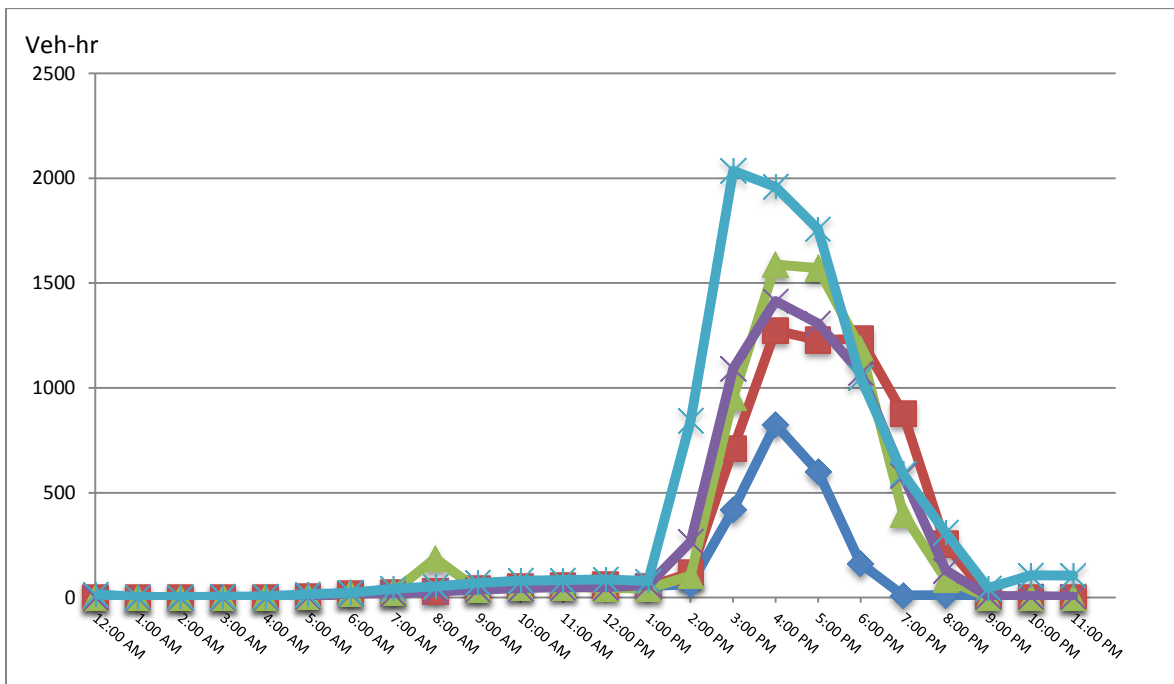


Figure 3-1. (a) SR-91 Eastbound weekday toll rate (July 2014) (b) Average delay of SR-91 Eastbound weekday (July 2014)

REAL-TIME PRICING BASED ON TRAFFIC CONDITIONS ON THE MANAGED LANES AND/OR GENERAL PURPOSE LANES

Analytical Models

Problem Formulation

Let $A(t)$ be the cumulative number of vehicles at time t that has entered a freeway segment containing a managed lane (ML) entrance. All vehicles were bound for a single destination past a general purpose lane (GPL) bottleneck of capacity μ_0 , which might be bypassed by paying a toll $\pi(t)$ to use an ML that has a bottleneck of capacity μ_1 ; see Figure 3-2.

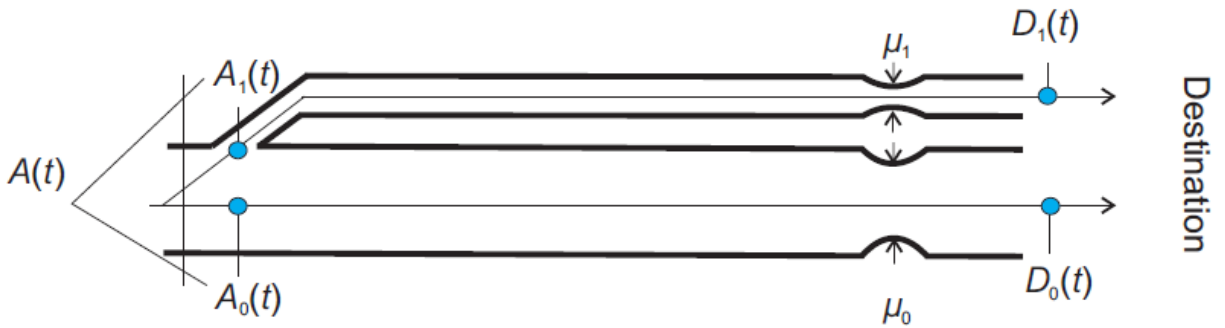


Figure 3-2. Schematic representation of the network

The cumulative count curve of vehicles using route r ($r=0$ for the GPL and $r = 1$ for the ML) was denoted $A_r(t)$ and the flow, $\lambda_r(t) = \dot{A}_r(t)$. Clearly,

$$\lambda(t) = \lambda_0(t) + \lambda_1(t), \quad (1)$$

and was assumed unimodal. Let $\tau_r(t)$ be the trip time in route r experienced by a user arriving at time t :

$$\tau_r(t) = \tau_r + w_r(t), \quad (2)$$

where τ_r is the free-flow travel time, and $w_r(t)$ is the queuing delay, which is expressed as:

$$w_r(t) = \frac{A_r(t) - A_r(t_r)}{\mu_r} - (t - t_r), \quad t_r < t < T_r \quad (3)$$

where t_r and T_r represent the times when route r begins and ends being congested, respectively.

Let:

$$\Delta = \tau_0 - \tau_1 \quad (4)$$

be the extra free-flow travel time for using the free alternative. Although in many cases one would expect $\tau_0 \approx \tau_1$, this was not assumed for maximum generality. It was convenient, however, to fix the sign of Δ now to simplify the exposition. We assumed that $\Delta > 0$; the other two cases are discussed in the last section of this paper. Under this assumption, we showed that $t_1 < t_0$ in the SO solution, i.e. the ML was used at capacity before the GPL, as shown next.

System Optimum

The SO solution is presented in Figure 3-3, which shows the system input-output diagram using total arrivals $A(t) = A_0(t) + A_1(t)$ and total virtual departures $D^*(t)$. The area between these curves is the total system delay, i.e. the total time spent queuing in the system. The method to obtain the curve $D^*(t)$ was introduced in Muñoz and Laval (2006), and was best visualized by imagining a ring connected to the rightmost end of $D^*(t)$ that is slid along $A(t)$ from right to left until $D^*(t)$ “touches” $A(t)$ again (at point “1” in the figure). This point corresponds to the time when both alternatives start being used at capacity (t_0 in our case since $\Delta > 0$, and $\lambda(t_0) = \mu_0 + \mu_1$), and from here one can identify the arrival time of the last vehicles to experience delay in each

alternative, T_r ($r = 0, 1$), and the time when the shorter alternative starts being used at capacity, (t_1 in our case, and $\lambda(t_1) = \mu_1$); see Figure 3-3. This figure also shows how to obtain the total system departure curve $D(t)$, which gives the count of vehicles reaching the destination at time t . Notice that total arrivals and departures in the system are not first-in-first-out. The resulting flow pattern is summarized below (Muñoz and Laval (2006)):

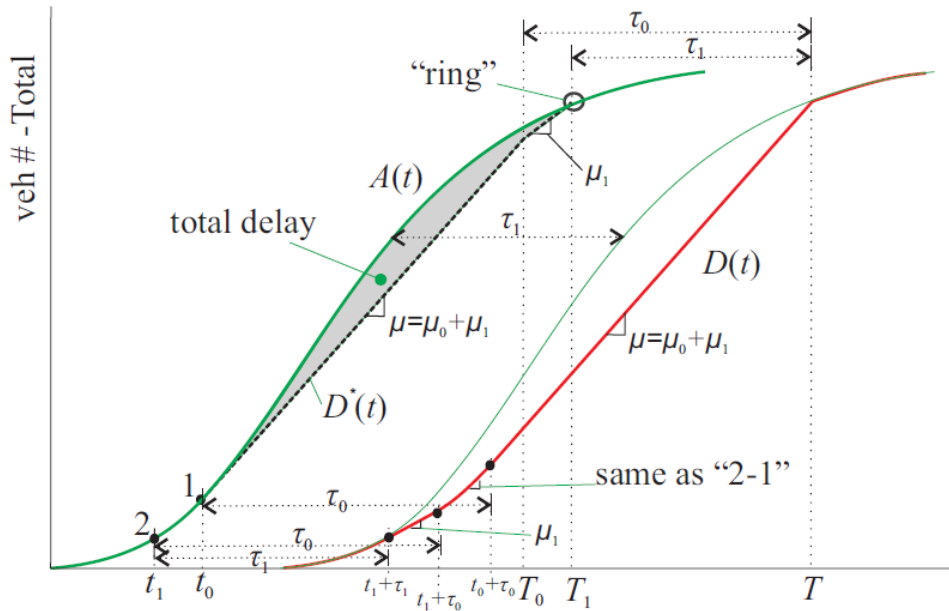


Figure 3-3. System optimum input-output diagram

System Optimum Conditions: The SO assignment when $\Delta > 0$ for users arriving at t satisfy:

1. $0 \leq t \leq t_1$: everybody chooses the ML
2. $t_1 \leq t \leq t_0$: the ML is used at capacity, excess inflow uses the GPL
3. $t_0 \leq t \leq T_0$: both alternatives are used at capacity
4. $t \geq T_0$: everybody chooses the ML

Note that these SO conditions say nothing about the alternative-specific arrivals $A_r(t)$; $r=0; 1$ in $t_0 \leq t \leq T_0$, which means that they are not unique in this time interval. Therefore, we focused on $t_0 \leq t \leq T_0$ because it is the only time interval where we have the flexibility to define $A_r(t)$. Without loss of generality and for simplicity we also set $t_0 = 0$; $A(t_0) = 0$. This implied that the delay to users arriving in $t < t_0$ was not considered. But this was irrelevant because such a delay was a constant of our problem, i.e. independent of the pricing strategy.

Setting $t_0 = 0$; $A(t_0) = 0$ simplified the construction of total arrivals and departures, as shown in Figure 3-4(a), and streamlined the derivation of alternative-specific input-output diagrams in Figures 3-4(b),(c), which are first-in-first-out. Recall that arrivals $A_r(t)$ are not unique; the only requirement is that they start at the origin, remain above the virtual departures, and pass through points “1” and “2” in Figures 3-4(b),(c), respectively. The departure curves at each alternative measured at the destination, $D_r(t)$, were obtained by shifting the virtual departures by the free-flow travel time r ; total system departures are then $D(t) = D_0(t) + D_1(t)$.

The total system cost is the area between total arrivals and departures, which is partitioned into the three components shown in Figure 3-4(a): (i) the total delay defined previously (area 0-4-3-0), (ii) the fixed travel time τ_1 incurred by all users (stripped area), and (iii) the extra travel time $\Delta \mu_0 T_0$ incurred by GPL users (lightly shaded area). It is seen that the stripped and slightly shaded areas in Figure 3-4(a) correspond to the sum of the respective areas in parts b and c of the figure.

Figures 3-4(b),(c) also show the delay, travel time and externality in each alternative, $w_r(t)$; $\tau_r(t)$ and $e_r(t)$, respectively. It is seen that:

$$e_r(t) = T - t - \tau_r(t). \quad (5)$$

The marginal cost $\tau_r(t)+e_r(t)$ in each alternative gives the extra cost incurred by the system if an additional unit of flow uses such alternative. In $t_0 \leq t \leq T_0$ the marginal cost was given by the time remaining until the end of congestion in the system, and it was identical on both alternatives, as expected. Outside this time interval, only the alternative with the least marginal cost (ML in this case) was used.

It was worth noting that point “2” in Figure 3-4(c) implies that at T_0 there has to be a queue in the ML, and therefore completely eliminating queues from the ML facility was not system optimal (when $\Delta > 0$). The reason was that starting at this time the GPL must not be used since its marginal cost was greater than the ML marginal cost.

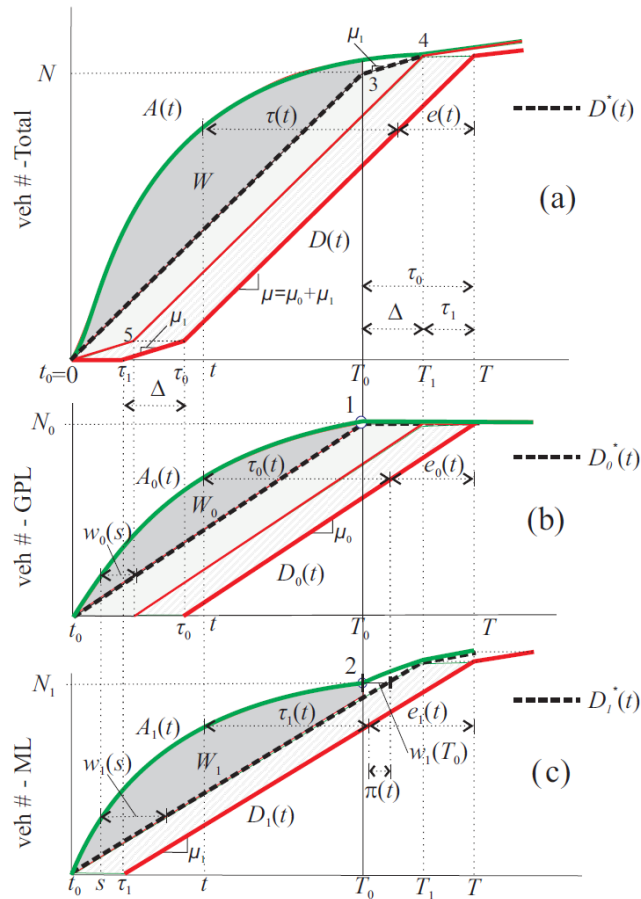


Figure 3-4. System optimum input-output diagram for users arriving at $t \geq t_0$

User Equilibrium with Pricing

The user equilibrium (UE) condition for our problem under any pricing strategy $\pi(t)$ —not necessarily SO tolls— was expressed as

$$\tau_0(t) = \tau_1(t) + \pi(t) \quad (6)$$

when both alternatives were used; otherwise, only the less expensive alternative was used.

Notice that in this formulation the toll had units of time, and implied that all users have the same value of time.

Following Laval (2009) it was more convenient to express the UE condition (6) in differential form, which equalized the rate of change in travel cost among alternatives, i.e. $\dot{\tau}_0(t) = \dot{\tau}_1(t) + \dot{\pi}(t)$, with $\dot{\tau}_r(t) = \frac{\lambda_r(t)}{\mu_r} - 1$, $r = 0,1$. This gave in our case:

$$\rho_0(t) = \rho_1(t) + \dot{\pi}(t), \quad (7)$$

where we have defined the demand-capacity ratios $\rho_r(t) = \frac{\lambda_r(t)}{\mu_r}$, $r = 0,1$. Notice that the differential UE condition was applicable only when the initial condition was in UE equilibrium.

Substituting (1) into (7) gave the UE assignment when both alternatives were used:

$$\rho_0(t) = \rho(t) + \bar{\mu}_1 \dot{\pi}(t), \quad (8a)$$

$$\rho_1(t) = \rho(t) - \bar{\mu}_0 \dot{\pi}(t), \quad (8b)$$

where $\mu = \mu_0 + \mu_1$ and $\bar{\mu}_r = \mu_r / \mu$ and $\rho(t) = \lambda(t) / \mu$ is demand-capacity ratio. It could be seen that for constant tolls, $\dot{\pi}(t) = 0$ the UE condition implied that each alternative and the system

had the same demand-capacity ratio. Arrival curves were obtained by integrating (8) from the time when both alternatives start being used, say t_{ini} , and thus:

$$A_r(t) = (-1)^r \bar{\mu}_0 \mu_1 (\pi(t) - \pi(t_{ini})) + \bar{\mu}_r A(t), \quad r=0,1. \quad (9)$$

where we have used $A(t_{ini})=0$ without loss of generality.

Properties of System Optimum Tolls

In this section, we identified and examined the properties of the SO toll, $\pi(t)$, that produced a SO assignment under UE. The goal of SO tolls was for every user to perceive the marginal cost it imposes on the system. This could be accomplished in our case by charging the externality in each alternative given by (5). Equivalently, since we wanted to maintain the GPL toll-free we only charged the difference in the externalities to the ML. This is illustrated in Figure 3-5(a), which shows the marginal cost in equilibrium along with travel times, delays, and externalities on each alternative, as a function of time. The figure also shows the SO flow pattern in each relevant time interval, with the exception of $t_0 \leq t \leq T_0$, where SO flows are not unique, and nor are $\tau_r(t)$ and $e_r(t)$. It followed that in the interval $t_0 \leq t \leq T_0$ the toll $\pi(t)$ was also not unique and could be chosen freely but within the following constraints:

(i) Boundary conditions constraints:

$$\pi(t_0) = \Delta, \quad \pi(T_0) = \Delta - w_1(T_0), \quad \text{and} \quad (10a)$$

(ii) Active bottleneck constraints:

$$\dot{\pi}(t) \geq \frac{\mu - \lambda(t)}{\mu_1}, \quad \text{if GPL at capacity with no queue} \quad (10b)$$

$$\dot{\pi}(t) \leq \frac{\lambda(t) - \mu}{\mu_0}, \text{ if ML at capacity with no queue} \quad (10c)$$

$$\frac{\lambda(t)}{\mu_1} \leq \dot{\pi}(t) \leq \frac{\lambda(t)}{\mu_0}, \text{ if } w_r(t) > 0, r = 1, 0 \quad (10d)$$

The boundary condition constraints (10a)–depicted as points “1” and “2” in Figure 3-5(b)–are a consequence of the SO conditions in the time intervals $t \leq t_0$ and $t \geq T_0$, which force pricing to be either fixed or arbitrary. Before t_1 , there was no congestion and therefore as long as $\pi(t) \leq \Delta$ all drivers choose the ML, as required by the SO condition. This is shown in Figure 3-5(b) by the shaded rectangles, which indicates that the toll could be anywhere inside this area. During the time interval $t_1 \leq t \leq t_0$ the ML has to operate at capacity with no queues while the excess demand should be diverted to the GPL, which is achieved using $\pi(t) = \Delta$. After T_0 only the ML should be used, which is achieved, again, by pricing within the shaded area in the figure.

The active bottleneck constraints (10b), (10c) and (10d) ensure that the bottlenecks are used at capacity in $t_0 \leq t \leq T_0$ and under all situations. In particular, if there is no queue on alternative r one should impose $\lambda_r(t) \geq \mu_r$ in (8a) or (8b), which gives (10b) or (10c). If there is a queue on both alternatives, the less restrictive condition $\lambda_r(t) \geq 0$ should be imposed, which gives (10d).

Delays

The Total delay for users arriving in $t_0 \leq t \leq T_0$, $W = \int_{t_0}^{T_0} (A(t) - \mu t) dt$, was a constant in our problem and was given by the dark shaded area in Figure 3-4(a). The delay in each alternative, $W_r(\pi) = \int_{t_0}^{T_0} (A(t) - \mu_r t) dt$, were functions of the pricing strategy. Using (9) gives:

$$W_r(\pi) = \int_{t_0}^{T_0} (-1)^r \bar{\mu}_0 \mu_1 (\pi(t) - \Delta) + (\bar{\mu}_r A(t) - \mu_r t) dt, \quad (11a)$$

$$= (-1)^r \bar{\mu}_0 \mu_1 \int_{t_0}^{T_0} (\pi(t) - \Delta) dt + \bar{\mu}_r W \quad (11b)$$

where one can see that $W = W_0(\pi) + W_1(\pi)$, as expected. It was interesting to note that manipulation of (11b) gives

$$\frac{W_0(\pi)}{\mu_0} - \frac{W_1(\pi)}{\mu_1} = \int_{t_0}^{T_0} (\pi(t) - \Delta) dt, \quad (12)$$

which could also be verified in Figure 3-5(a). In this figure, the shaded areas correspond to

$$\int_{t_0}^{T_0} w_r(t) dt = \int_{t_0}^{T_0} \frac{\mu_r w_r(t) dt}{\mu_r} = \frac{W_r}{\mu_r}, r = 0, 1, \text{ respectively.}$$

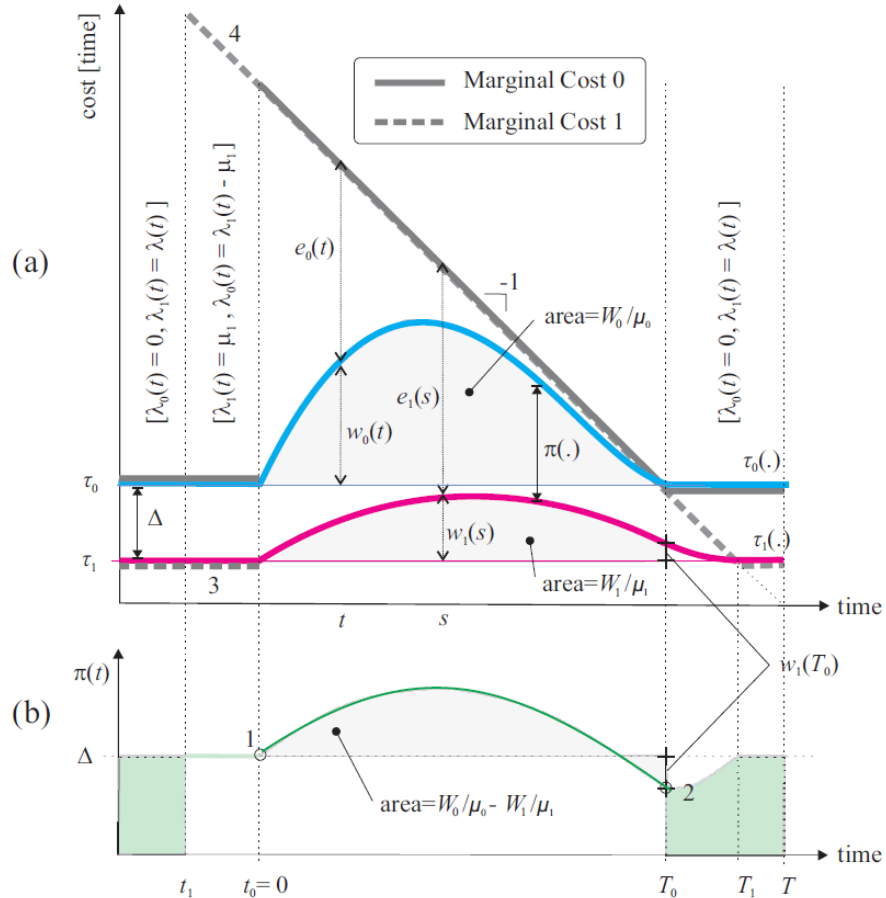


Figure 3-5. Evolution of the system (a) marginal cost, externality, travel time and (b) toll

Revenue

Let $R(\pi)$ be the revenue under strategy $\pi(t)$. It could be expressed as $\int_{t_0}^{T_0} \lambda_1(t)\pi(t)dt$,

which by (8b) is also:

$$R(\pi) = \bar{\mu}_1 \int_{t_0}^{T_0} \lambda_1(t)\pi(t)dt - \bar{\mu}_0\mu_1 \int_{t_0}^{T_0} \dot{\pi}(t)\pi(t)dt, \quad (13a)$$

$$= \bar{\mu}_1 \int_{t_0}^{T_0} \lambda_1(t)\pi(t)dt - C \quad (13b)$$

where $C = \bar{\mu}_0\mu_1(\Delta^2 - (\Delta - w_1(T_0))^2)/2$ was a constant that follows from $\int_{t_0}^{T_0} \dot{\pi}(t)\pi(t)dt = 1/2\pi(t)^2|_{t_0}^{T_0}$ and (11a). Therefore, maximizing revenue could be expressed as the following mathematical program:

$$\max_{\pi(t)} \int_{t_0}^{T_0} \lambda(t)\pi(t)dt, \text{ subject to (10),} \quad (14)$$

and we have the following result:

Result. (*Maximum Revenue*) Revenue is maximized for the highest possible $\pi(t)$ that does not violate the SO condition; i.e., the ML is maintained at capacity with no queues for as long as possible (see Figure 3-6(a)).

Proof : Maximizing $\int_{t_0}^{T_0} \lambda(t)\pi(t)dt$ is equivalent to maximizing $\int_{t_0}^{T_0} \pi(t)dt$ because (i) $\lambda(t)$ is exogenous and nonnegative, and (ii) the active bottleneck constraints are in terms of $\dot{\pi}(t)$, which means that the highest possible $\pi(t)$ value at a given time t is obtained only if it is preceded by the highest possible $\pi(t')$ value at an earlier time t' . Therefore, the optimal solution is obtained in a (t, π) diagram starting from each boundary point (t_0, Δ) and $(T_0, \Delta - w_1(T_0))$, and drawing

HOT Lanes Under Linear Tolls

System optimum tolls on HOT lanes could be characterized within the proposed framework using $\Delta = 0$; typically $\mu_1 \ll \mu_0$ but we did not need this assumption. For simplicity and without loss of generality we neglected high occupancy vehicles (who do not pay the toll to use the HOT lane) in this analysis. The reader can verify using Figure 3-4 that in this case $w_1(T_0) = 0$, and therefore the boundary condition (10a) changes to:

$$\pi(t_0) = 0, \pi(T_0) = 0 \quad (15)$$

We showed that when the pricing strategy is linear, as defined momentarily, we obtained closed-form expressions for revenue, delay, and flows. It turned out that these quantities were all linear functions of a single parameter, which made the optimization of this system very simple, to the point where the appropriate pricing strategy to accomplish a given objective was reduced to choosing a single parameter value.

Tolls Linear In the Arrivals

We assumed that tolls are linear (in the total arrival curve) if there is a constant, a , called the pricing coefficient, such that:

$$\dot{\pi}(t) = (\rho(t) - 1)a, \quad t_0 \leq t \leq T_0, \quad (16)$$

or equivalently (letting $t_0=0$),

$$\pi(t) = \frac{(A(t) - \mu t)a}{\mu}, \quad t_0 \leq t \leq T_0, \quad (17)$$

Which means that the toll is proportional to the system queue $A(t) - \mu t$, or to the delay $w(t) = (A(t) - \mu t) / \mu$; see Figure 3-4(a). Notice that a is dimensionless. This strategy is “real-time” because from

(10) it is clear that to determine the toll at time t , all that needed is the demand-capacity ratio at the same time, which is measured in real-time.

Result: *Assignment, delays, and revenues under linear tolls*

Under linear pricing the flow assigned to each alternative, delays and revenue are linear functions of the pricing coefficient; i.e., in dimensionless form:

$$\rho_0(a, t) = (1 + a\bar{\mu}_1)\rho(t) - a\bar{\mu}_1, \quad t_0 \leq t \leq T_0, \quad (18a)$$

$$\rho_1(a, t) = (1 - a\bar{\mu}_0)\rho(t) + a\bar{\mu}_0, \quad t_0 \leq t \leq T_0, \quad (18b)$$

$$\frac{W_0(a)}{W} = (1 + a\bar{\mu}_1)\bar{\mu}_0, \quad (18c)$$

$$\frac{W_1(a)}{W} = (1 - a\bar{\mu}_0)\bar{\mu}_1, \quad (18d)$$

$$\frac{R(a)}{W} = a\bar{\mu}_1, \quad (18e)$$

Proof : For the flow assigned to each alternative, combining (8) and (16) gives the desired result.

For the delays, we notice that on alternative r it is given by (11b) using $\int_{t_0}^{T_0} \pi(t)dt = aW/\mu$,

which follows from (17), and simplifies to (18c) and (18d) as sought. In the case of the revenue,

from Result of the maximum revenue, the revenue is proportional to $\int_{t_0}^{T_0} \lambda(t)\pi(t)dt$, which

integrated by parts gives:

$$\int_{t_0}^{T_0} \lambda(t)\pi(t)dt = A(t)\pi(t)|_{t_0}^{T_0} - \int_{t_0}^{T_0} \lambda(t)\dot{\pi}(t)dt \quad (19a)$$

$$= a \int_{t_0}^{T_0} A(t)\left(1 - \frac{\lambda(t)}{\mu}\right)dt, \quad (19b)$$

$$= a\left(\int_{t_0}^{T_0} A(t)dt - 1/2A(T_0)T_0\right) \quad (19c)$$

$$= aW \quad (19d)$$

The first term in (19a) is zero because of (15), while (19c) results from $\int A(t)\lambda(t)dt = A(t)^2/2$ and noting that $A(T_0) = \mu T_0$. The revenue is obtained by substituting (19d) into (13), which gives (18e).

It is interesting to note that all relevant measures of performance in our problem are not only a linear function of a single parameter, a , but also linear functions of all the constants that define the problem: $\bar{\mu}_0$, $\bar{\mu}_1$ and W .

Imposing nonnegative delays gives the bounds for the pricing coefficient:

$$a_{max} = \frac{1}{\bar{\mu}_0}, \quad a_{min} = -\frac{1}{\bar{\mu}_1}, \quad (20)$$

which also are derived by imposing $\rho_0(t) \geq 1$ for a_{min} and $\rho_1(t) \geq 1$ for a_{max} . Since the revenue is a linearly increasing function of a , it follows that the maximum revenue is $R(a_{max})$, namely:

$$R_{max} = \frac{\bar{\mu}_1}{\bar{\mu}_0} W. \quad (21)$$

Replacing $a = a_{max}$ in (18) shows that maximum revenue implies the HOT lane is used at capacity with no queues.

Optimizing operator objectives

Since all performance measures became analytical under linear pricing, it was a simple matter to optimize any particular objective set by the operator. For example, it followed from Results of Assignment, delays and revenues under linear tolls that any objective function $f(\cdot)$ that is a linear combination of delays and revenue, e.g.:

$$f(a) = c_0W_0(a) + c_1W_1(a) + R(a), \quad \text{with } c_0, c_1 = \text{constants}, \quad (22)$$

was also a linear function of the pricing coefficient. Therefore, the optimal solution was either a_{min} , a_{max} or an arbitrary value within these bounds, depending on the sign of $f'(a) = \bar{\mu}_1W(1 + \bar{\mu}_0(c_0 - c_1))$. Of course, nonlinear objectives were also possible but the optimal reduced to finding the extreme of a scalar function.

Another type of objective could be maximizing revenue while ensuring that the GPL delay does not exceed the HOT lane delay by a factor of, say, r ; i.e.: $\max_a R(a)$ subject to $W_0(a) \leq rW_1(a)$. Since $R(a)$ is a linearly increasing function of a , the optimum a , namely a^* , is the highest possible value of a , which in this case is given by the condition $W_0(a^*) = rW_1(a^*)$, or:

$$a = \frac{\bar{\mu}_1 r - \bar{\mu}_0}{\bar{\mu}_0 \bar{\mu}_1 (1+r)} \quad (23)$$

provided that it is not larger than $a_{max} = 1/\bar{\mu}_0$. The corresponding revenue $R(a^*)$ was given by (18e), which could be written as $R(a^*) = (r - \frac{\mu_0}{\mu_1})/(1 + r)R_{max}$. This implied that under this policy, revenue decreases by a factor of $= (1 + r)/(r - \frac{\mu_0}{\mu_1})$ compared to the maximum revenue policy.

Other real-time pricing strategies

It turned out that a wide family of real-time pricing strategies that may arise in practice are linear in the arrivals and therefore share the properties outlined in the preceding section. In these strategies, tolls were calculated as linear functions of the traffic conditions on (i) the HOT lane, (ii) the GPL, and/or (iii) all lanes. Table 3-1 summarizes cases that the traffic condition is the delay or the number of vehicles in queue.

Table 3-1. Pricing strategies summary

Toll linear in	$\pi(t)$	$\lambda_0(t)/\mu_0$	c_{\min}	c_{\max}	a
ML queue	$c(A_1(t) - \mu_1 t)$	$\frac{\lambda(t) + c\mu_1(\lambda(t) - \mu_1)}{\mu + c\mu_0\mu_1}$	$-\frac{\mu}{\mu_1(\mu_0 + \mu\mu_1)}$	∞	$\frac{c\mu_1\mu}{\mu + c\mu_0\mu_1}$
GPL queue	$c(A_0(t) - \mu_0 t)$	$\frac{\lambda(t) - c\mu_0\mu_1}{\mu - c\mu_0\mu_1}$	$-\frac{\mu}{(\mu - 1)\mu_0\mu_1}$	$1/\mu_0$	$\frac{c\mu\mu_0}{\mu - c\mu_0\mu_1}$
Queue on All lanes	$c(A(t) - \mu t)$	$\frac{\lambda(t) + c(\lambda(t) - \mu)\mu_1}{\mu}$	$-1/\mu_1$	$1/\mu_0$	$c\mu$
ML delay	$c\left(\frac{A_1(t)}{\mu_1} - t\right)$	$\frac{\lambda(t)(1+c) - c\mu_1}{\mu + c\mu_0}$	$-\frac{\mu}{\mu_0 + \mu\mu_1}$	∞	$\frac{c\mu}{\mu + c\mu_0}$
GPL delay	$c\left(\frac{A_0(t)}{\mu_0} - t\right)$	$\frac{\lambda(t) - c\mu_1}{\mu - c\mu_1}$	$-\frac{\mu}{(\mu - 1)\mu_1}$	1	$\frac{c\mu}{\mu - c\mu_1}$
Delay on All lanes	$c\left(\frac{A(t)}{\mu} - t\right)$	$\frac{\mu_0(\lambda - c\mu_1) + \mu_1(\lambda + c(\lambda - \mu_1))}{\mu^2}$	$-\frac{\mu}{\mu_1}$	$\frac{\mu}{\mu_0}$	c

This result extends to any traffic condition that is a linear function of the delay in each alternative $w_r(t)$. They included the number of vehicles in the queue $\mu_r w_r(t)$, travel time $\tau_r + w_r(t)$, pace $(\tau_r + w_r(t))/L$, density $k(t) = k_c + \mu_r w_r(t)/L$; if we assume a linear congestion branch in the flow-density relationship one may also include the flow in congestion $q(t) = \frac{\kappa - k(t)}{w}$, where κ is the jam density and $-w$ is the wave speed. The only difference is the way each one would be implemented in practice. Each strategy would keep track of different traffic variables, such as queue length, delay, density, etc. An operator should choose to track the traffic variables that are measured more accurately with the available technology. In most cases, it is more reliable to estimate speeds so that a delay-based strategy may be advisable.

Numerical Example

To illustrate our method, consider the HOT problem with the parameter values shown in Figure 3-7. Tolls are given by (17) and the traffic assignment by (18a), (18b). Figure 3-7(a) illustrate the cases $a = a_{max}$ ($=1.25$) and a given by (23), which correspond to the scenario of maximum revenue under no constraints, and Figure 3-7(b) depicts the scenario of constrained maximum revenue such that the GPL delay does not exceed the HOT lane delay by a factor of $r = 5$ (i.e. $a = a^*$ ($= 5/24$)). Parameter values are $\mu_0=9,600$ vph, $\mu_1=2,400$ vph, $\tau_0 = \tau_1 = 0.25$ hr ($\Delta= 0$); the arrival rate $\mu(t)$ is 18,000 vph in $0 < t < 1$ hr, and 2,400 vph in $t > 1$ hr, where $t_1 = t_0 = 0$ hr. It could be seen that in the unconstrained scenario, the GPL users experience all the delay while HOT users enjoy no queues, as expected. In contrast, in the constrained scenario both alternatives are congested with $W_0/W_1 = 5$, and the revenue decreases by a factor of 6, as expected. Notice in part e of the figure that the system input-output diagram for both scenarios is identical, which illustrates that two different pricing strategies yield the same SO solution.

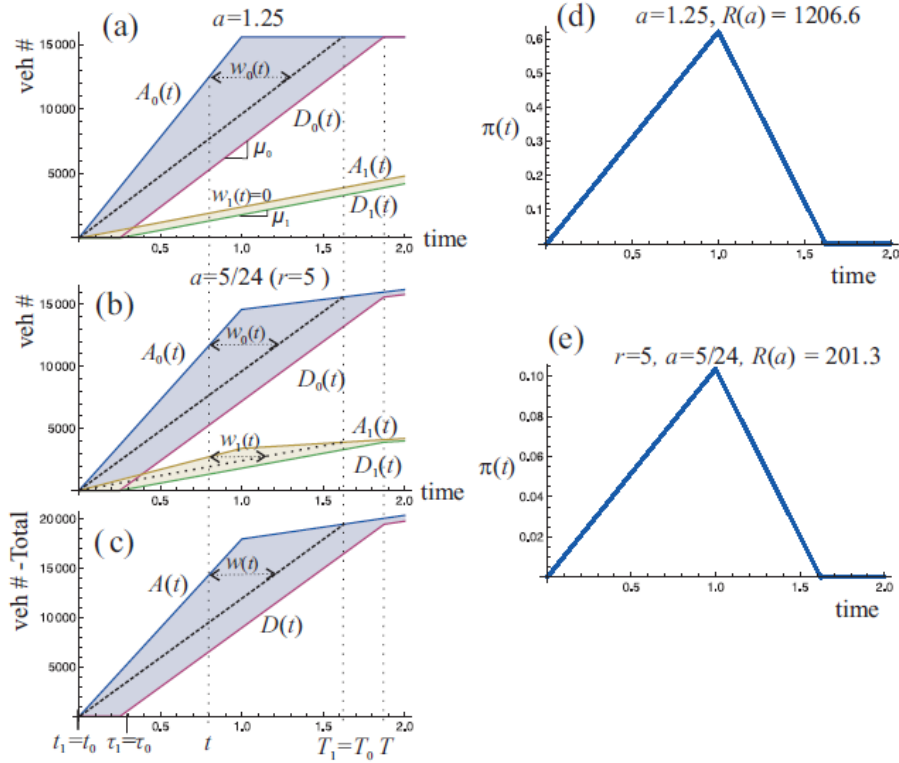


Figure 3-7. Input-output diagram for scenario of (a)maximum revenue under no constraints, (b)maximum revenue constrained, and (c)system; (d) and, (e) tolls corresponding to (a) and (b)numerical example

VARIABLE BOTTLENECK CAPACITY LINEAR TOLL PRICING

In the real-time linear toll pricing strategy, we assumed that the bottleneck capacity (μ_0, μ_1) of general purpose lanes and managed lanes are constant. However, in reality the bottleneck capacity varies with the dynamics of traffic congestion. In this section, we relaxed this assumption and developed traffic assignment model. In this variable bottleneck capacity model, the predictive travel time was calculated based on the bottleneck capacity at current time $t, \mu(t)$, as in Figure 3-8.

$$\tau(t) = \frac{A(t)-D(t)}{\mu(t)} \quad (24)$$

The predicted travel time was the simplest estimation for vehicles arriving at time t , but had an obvious prediction error; see Figure 3-8.

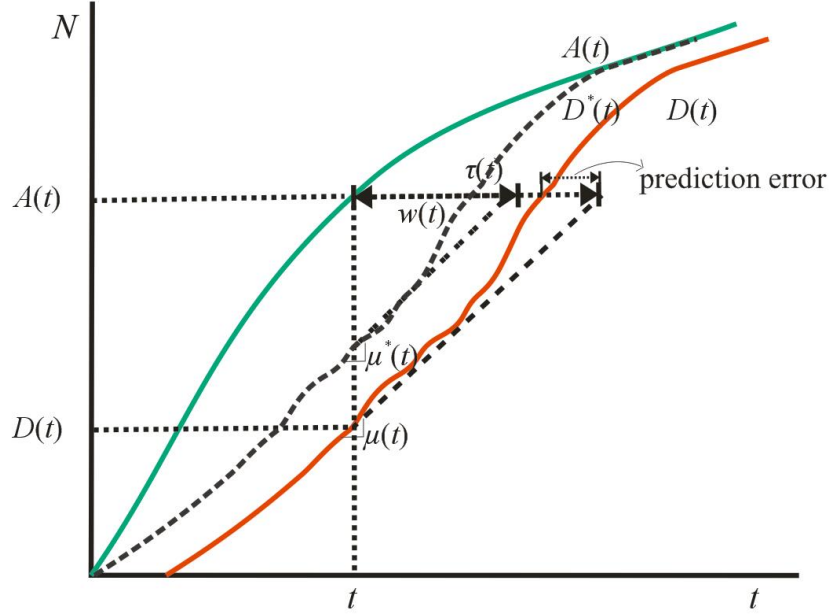


Figure 3-8. Input-output diagram of variable bottleneck capacity linear toll pricing strategy

In the variable bottleneck capacity model, the real-time linear toll is now expressed as:

$$\pi(t) = aw(t) = a \frac{A(t) - D^*(t)}{\mu^*(t)}, \quad (25)$$

where $D^*(t)$ and $\mu^*(t)$ are virtual departure and virtual departure rate, and assuming that $\mu(t) \approx \mu^*(t)$, the toll is proportional to the predicted delay at time t . Combining (24) and (25) into UE condition (6) in differential form gives us the following traffic assignment equations:

$$\rho_0(t) = \rho(t) + \bar{\mu}_1(t)\dot{\pi}(t) + \frac{\tau_0(t)}{\mu_0(t)}\bar{\mu}_1(t)\dot{\mu}_0(t) - \frac{\tau_1(t)}{\mu(t)}\dot{\mu}_1(t) \quad (26a)$$

$$\rho_1(t) = \rho(t) - \bar{\mu}_0(t)\dot{\pi}(t) + \frac{\tau_1(t)}{\mu_1(t)}\bar{\mu}_0(t)\dot{\mu}_1(t) - \frac{\tau_0(t)}{\mu(t)}\dot{\mu}_0(t) \quad (26b)$$

$$\text{where } \dot{\pi}(t) = \frac{a((\lambda(t)-\mu^*(t))\mu^*(t)-(A(t)-D^*(t))\mu^*(t))}{\mu^*(t)^2} = a(\rho^*(t) - 1) - \pi(t) \frac{\dot{\mu}^*(t)}{\mu^*(t)} \quad (26c)$$

Unfortunately, it was not easy to derive analytical solutions of delays and revenue. Therefore, we introduced a simulation method to analyze delays and revenues of the variable bottleneck capacity real-time linear toll model.

COMPARISON TO FIXED TOLL PRICING

The fixed toll was the simplest pricing method, but the toll needed to be reasonable to fully utilize the managed lane. Under the fixed toll pricing, the ML was used only when the toll was beneficial. Under UE, drivers used the ML only if the toll was equal to or less than the difference between the travel time of GPL and the ML, i.e.

$$\tau_0(t) - \tau_1(t) \geq \pi \quad (27)$$

If the condition was met, the traffic was allocated based on the UE assignment (28) as in (8) (s.t. $\dot{\pi}(t) = 0$); i.e.:

$$\rho_0(t) = \rho_1(t) = \rho(t), \quad (28)$$

The fixed toll pricing model was interpreted as Laval (2009)'s User Optimum equilibrium, where the fixed toll was the same as Δ_r^* in the paper, which is “a constant travel time-independent of flow incurred when taking off-ramp r .” In that paper, vehicles in freeway do not divert to off-ramp until delay of freeway was equal to the Δ_r^* . When the delay was as large as Δ_r^* , excess freeway demand diverts to the off-ramp, and when the off-ramp was also congested, traffic was assigned by rule (28). Therefore, under the fixed toll pricing, the capacity of managed lane was “wasted” until the GPL delay equals to the toll. Figure 3-9 depicts examples of the fixed toll

pricing scheme at three levels (π_a, π_b, π_c) and their input-output diagram. t_{xr} is the time that vehicles start using the managed lane with toll π_x , and T_{xr} is when congestion ends with toll π_x ($r=0$ GPL, $r=1$ ML).

The revenue of the fixed toll pricing is expressed as $\pi_r \times \int_{t_r}^{t_r^*} \lambda_1(t) dt$, and using (28),

$$R(\pi_r) = \pi_r \bar{\mu}_1 \int_{t_r}^{t_r^*} \lambda(t) dt \quad (29)$$

Delays are also expressed similarly, $W(\pi_r) = \int_{t_0}^{T_r} (A(t) - D(t)) dt$, where t_0 is the time when the GPL begins to be congested.

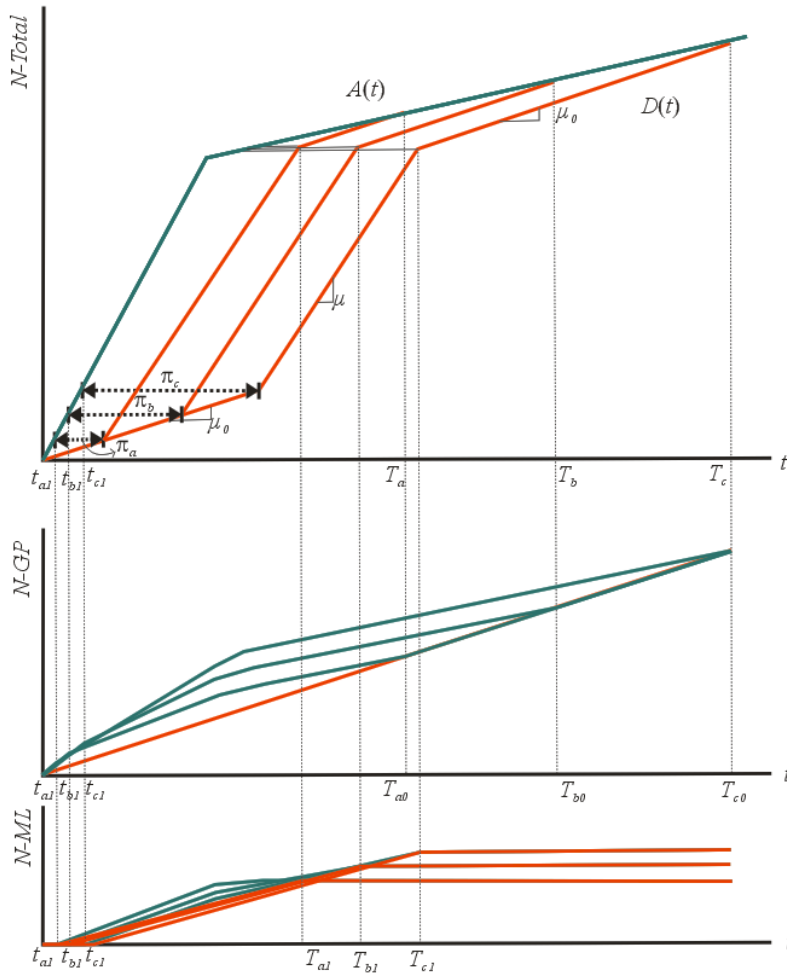


Figure 3-9. Input-output diagram of fixed toll pricing strategy at 3 different levels ($\pi_a < \pi_b < \pi_c$)

COMPARATIVE ANALYSIS USING SIMULATION

In this section, we compared fixed toll pricing strategy (FT), constant bottleneck capacity linear toll pricing strategy (CLT), and variable bottleneck capacity linear toll pricing strategy (VLT) using the simulation model.

It is well known that the existing off-the-shelf traffic simulation software are deficient in simulating congested traffic dynamics on freeways. This is mainly due to insufficient inbuilt models and limited flexibility to allow users to change the models. Georgia Tech has developed a micro-simulation application, called hereafter *GTsim*, which is based on the kinematic wave model. This application includes latest car following and lane changing models that replicate bounded vehicle accelerations, realistic lane change maneuvers, congestion dynamics such as capacity drop and lateral propagation of congestion. The latest mandatory lane change models used in *GTsim* also replicated spatially realistic lane changes and vehicle accumulations on a lane. *GTsim* was built in JAVA to perform faster than real-time simulation.

The network consists of two parallel roads, general purpose lanes and a High Occupancy Toll lane as in Figure 3-10. In the figure, traffics are heading eastbound, the top lane is the HOT lane (in blue), and other lanes are general purpose lanes (in red). HOT lane vehicles are inserted to the HOT lane directly at the input section, which prevent congestions forming in front of the HOT lane section. An exit ramp is set 1km downstream of the end of the HOT lane. In this way, mandatory lane changing maneuvers to exit the freeway from HOT lane users create a bottleneck of variable capacity. Figure 3-11 depicts the congestion formation on each lane. Green means free flow speed, and red, congested

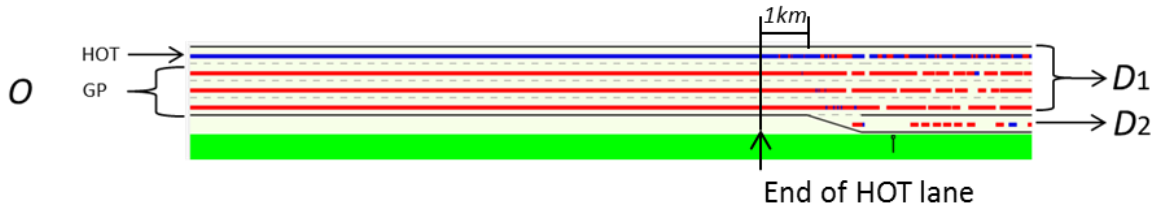


Figure 3-10. Diagram of simulation model

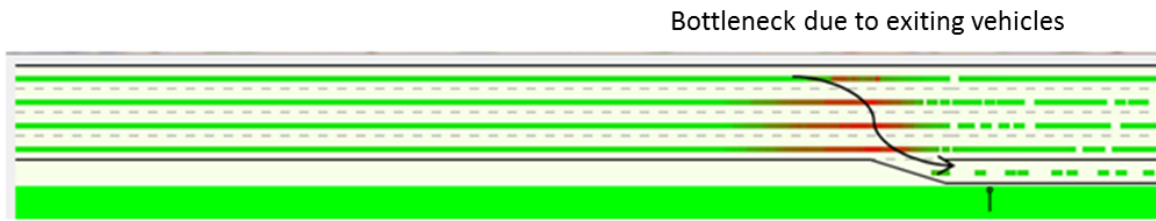


Figure 3-11. Congestion formation of the traffic in the simulation model

Traffic demand was set as follows: $\lambda(t)$ is 7,500vph in $t < 4,800s$, and 5,000vph in $t \geq 4,800s$. Note that ideal capacity (without Lane-changes) is 2,500vph/lane. Origin-Destination distribution and portions of through vehicles and exit vehicles are summarized in Table 3-2.

Table 3-2. O/D distribution of simulation

Time(s)		$D_1(vph)$	$D_2(vph)$	Exit Veh. Portion
$t < 4800$	O	6,000	1,500	1/5
$t > 4800$		4,000	1,000	1/5

We simulated two-hour experiments which contain the formation and dissipation of queues in all lanes. Tolls((17), (25)) and the ratio of HOT lane vehicle((18a,b), (26a,b), (28)) that to be inserted directly to the HOT lane were calculated every two minutes, which means that the toll was constant for two minute periods for all cases.

In the fixed toll pricing strategy (FT), we set the toll in units of time from $0.01hr$ to $0.1hr$ in $0.01hr$ interval (10 cases), and traffic was assigned using (28) under condition (27). Note that when the HOT lane bottleneck is inactive, $\mu_1(t)$ is equal to the ideal capacity.

In the constant bottleneck capacity linear toll pricing strategy (CLT), the toll was set using (17), by changing a parameter “ a ” with a range of $0.1\sim 1.0$ in 0.1 intervals (10 cases), and traffic assignments were followed by (18a, b). Although the bottleneck capacity μ_r changes in time every time-step, we name this strategy as the “constant” bottleneck capacity linear toll pricing strategy because equations (17, 18a, b) assumed that the bottleneck capacity is constant. In the variable bottleneck capacity linear toll pricing strategy (VLT), the toll was decided by (25), also by changing a parameter “ a ” with a range of $0.1\sim 1.0$ in 0.1 interval (10 cases), and traffics were allocated from (26). Note that derivative of bottleneck capacity $\dot{\mu}_r(t)$ was calculated by Euler’s method.

In the following, we investigated the performances of each strategy in terms of social cost (delays) and benefit (revenue). Also, we verified our results with analytical equations whenever possible.

The total delay (in the unit of $veh-hr$) - which is composed of GP lanes’ delays (W_0) and HOT lane’s delays (W_1) - of each pricing strategy is summarized in Figure 3-12. It was found that for all ranges of the parameter a in the linear toll pricing strategies (CLT, VLT), the total delay was smaller than that of the fixed toll pricing strategy for all fixed tolls that we experimented. Note that in the fixed toll pricing strategy, the total delay tends to increase as the toll increases. This is explained by Figure 3-9 in the previous section. However, the total delays

of the linear toll pricing strategies seemed to be random in terms of the parameter a , which we assumed to be constant for all cases.

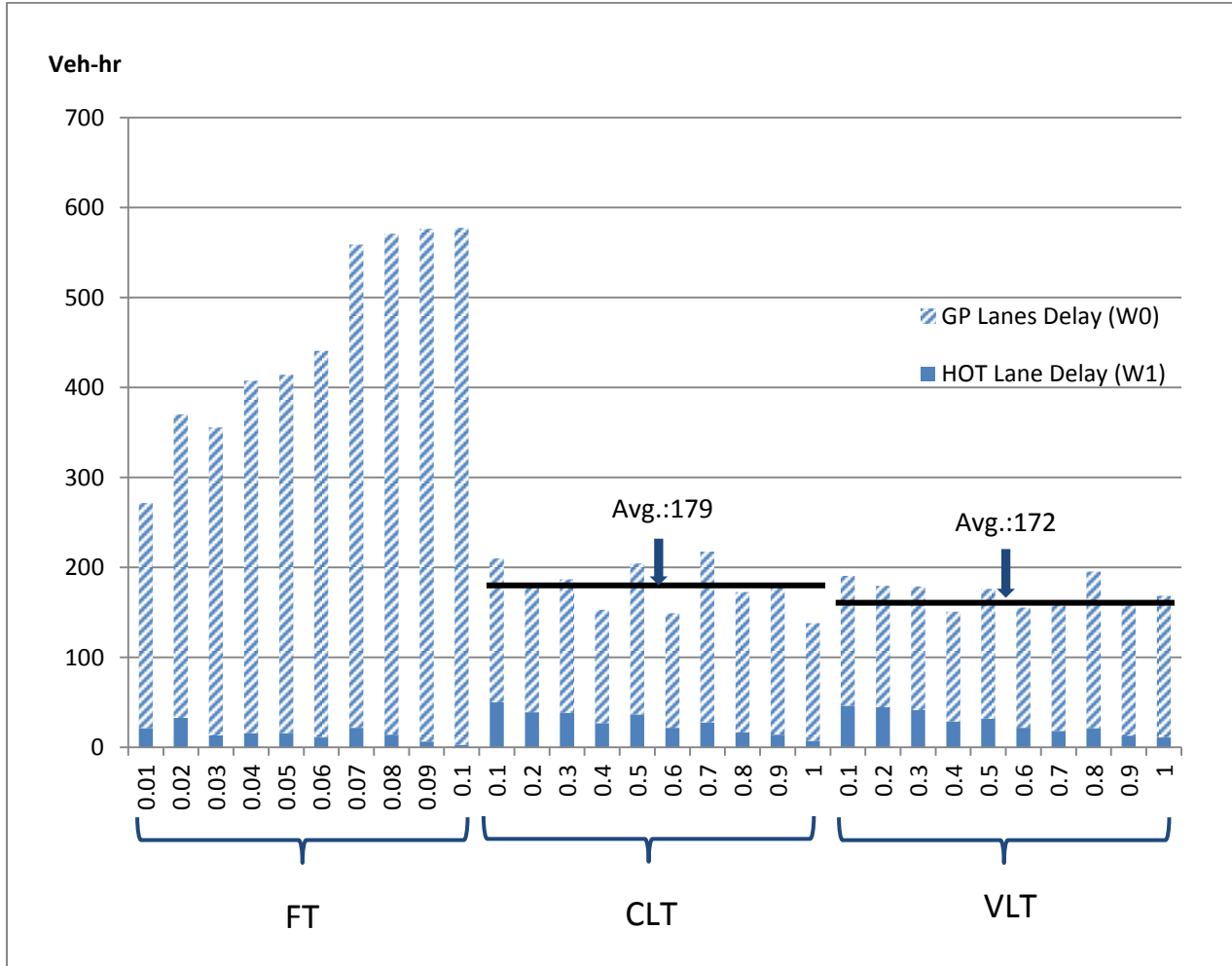


Figure 3-12. Total delays of pricing strategies

In Figure 3-12, it was interesting to note that HOT lane delays were decreasing as a parameter a increases in CLT and VLT strategies. This tendency reminded us of the equation (18d) of linear toll strategy. Converting (18d) into linear equation in terms of a :

$$\frac{w_1(a)}{w} = (1 - a\bar{\mu}_0)\bar{\mu}_1 = ac_1 + c_0 \quad (30)$$

To verify (30) with our results, we extracted average $\bar{\mu}_0, \bar{\mu}_1$ of each strategy for all cases as in Figure 3-13. Note that these values are measured when the bottleneck is active.

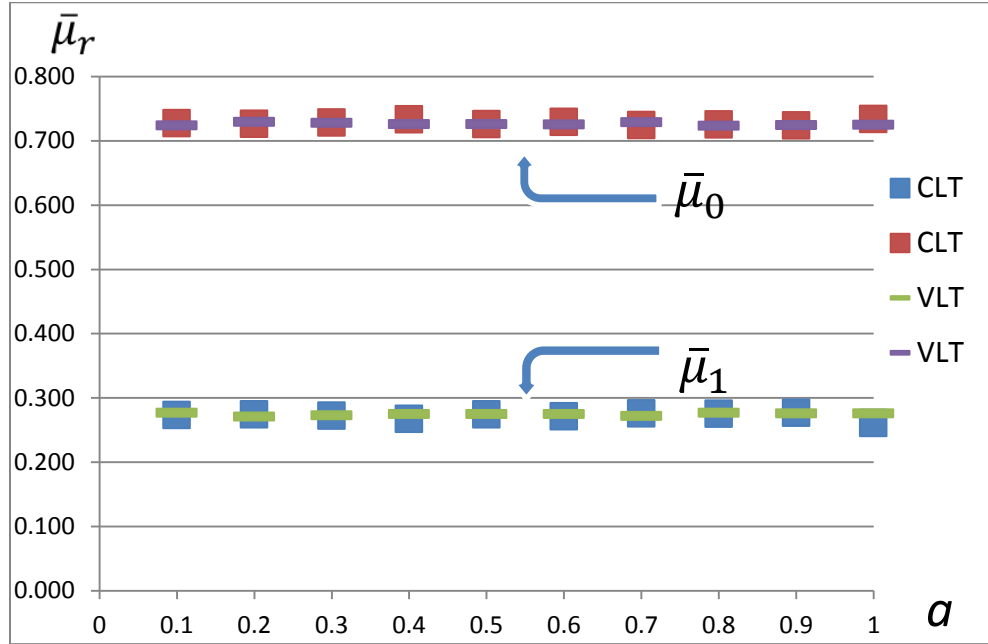


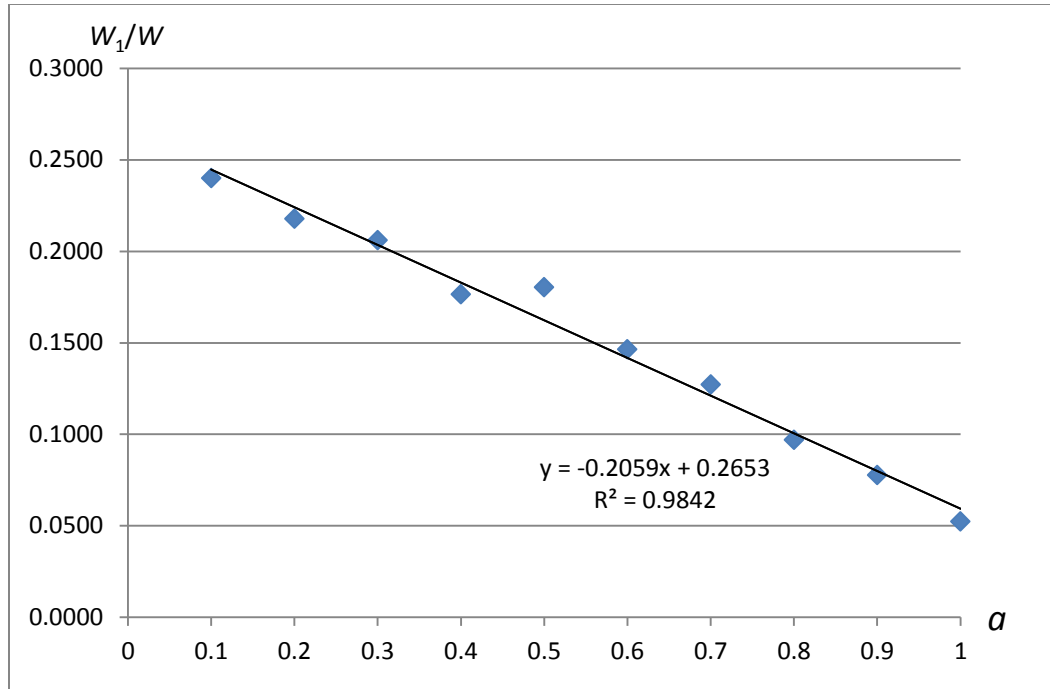
Figure 3-13. Average of $\bar{\mu}_0, \bar{\mu}_1$ in CLT and VLT when bottleneck is active

Average $\bar{\mu}_0$ and $\bar{\mu}_1$ of all cases in CLT and VLT were 0.7276, 0.2718 and 0.7257, 0.2743 respectively. After substituting these numbers into (30), and obtaining coefficients of linear regression equations of simulation data as Figure 3-14(a) and (b), we compared 95% confidence intervals of coefficients; see Table 3-3.

Table 3-3. Comparing equation (30) and simulation results

		95% C.I. c_1	95% C.I. c_0
CLT	eq.(30)	(-0.2035, -0.1919)	(0.2603, 0.2833)
	Simulation	(-0.2272, -0.1846)	(0.2521, 0.2785)
VLT	eq.(30)	(-0.2010, -0.1969)	(0.2697, 0.2789)
	Simulation	(-0.2510, -0.1932)	(0.2653, 0.3011)

(a) CLT



(b) VLT

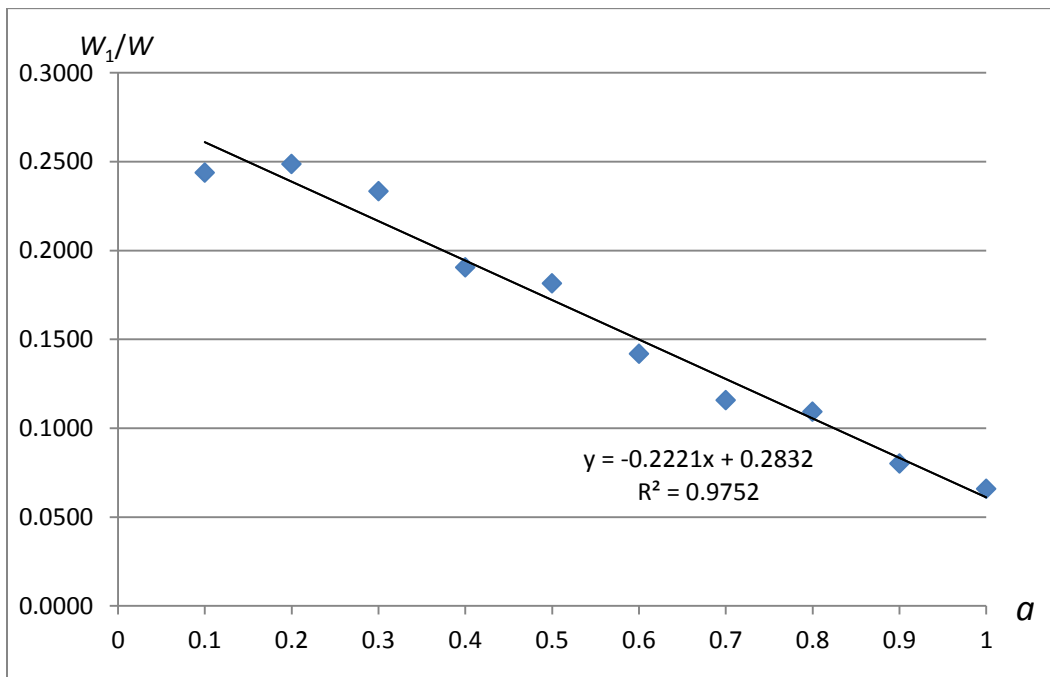


Figure 3-14. Relations of W_1/W and a in (a) CLT and (b) VLT

Revenue for each pricing strategy is summarized in Figure 3-15. Note that revenue is calculated by multiplying the number of HOT lane users and tolls paid by the users. As the toll in our experiment has the unit of time, the unit of the revenue is *veh-hr*.

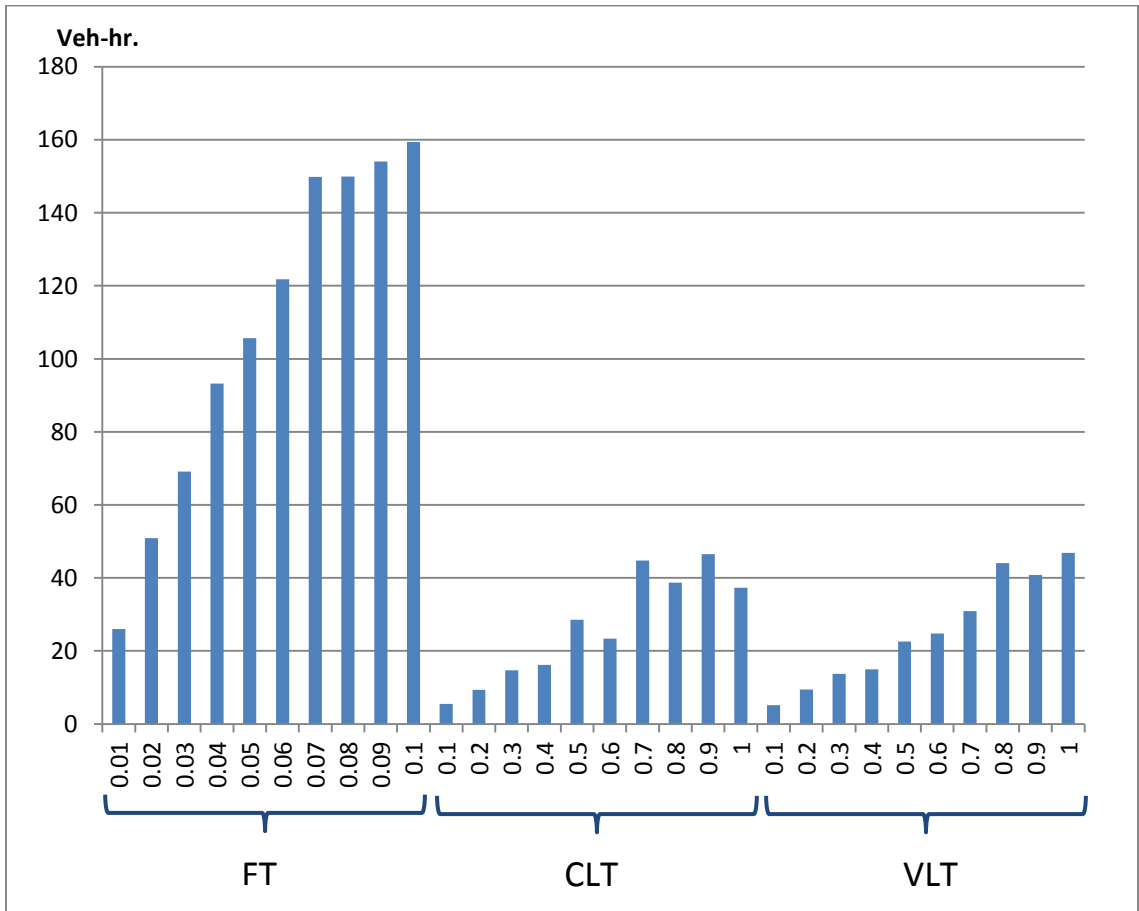


Figure 3-15. Revenues of pricing strategies

It was found that the revenue of the fixed toll pricing strategy was always larger than the revenue of other linear pricing strategies except the fixed toll is 0.01 *hr*. Specifically, the maximum revenue of the fixed toll pricing strategy lied in when the fixed toll is the largest, i.e. 0.1 *hr*, and that revenue was more than three times of the maximum revenue of linear pricing strategies. Also, revenues of all pricing strategies tended to increase as the toll and parameter *a*

increase. It was reasonable to assume that for a state-operated HOT lane, the total delay (W) is a social cost and the revenue (R) is a benefit. The benefit-cost ratio (B/C) in our experiments is given by equation (18e) in the linear toll pricing.

$$\frac{R(a)}{W} = a\bar{\mu}_1 \quad (18e)$$

A relation between R/W ratios of the fixed toll pricing and the fixed toll π is depicted in Figure 3-16 below. As in the figure, the below quadratic function is detected from the data:

$$R/W = -39.114\pi^2 + 6.1286\pi + 0.0396$$

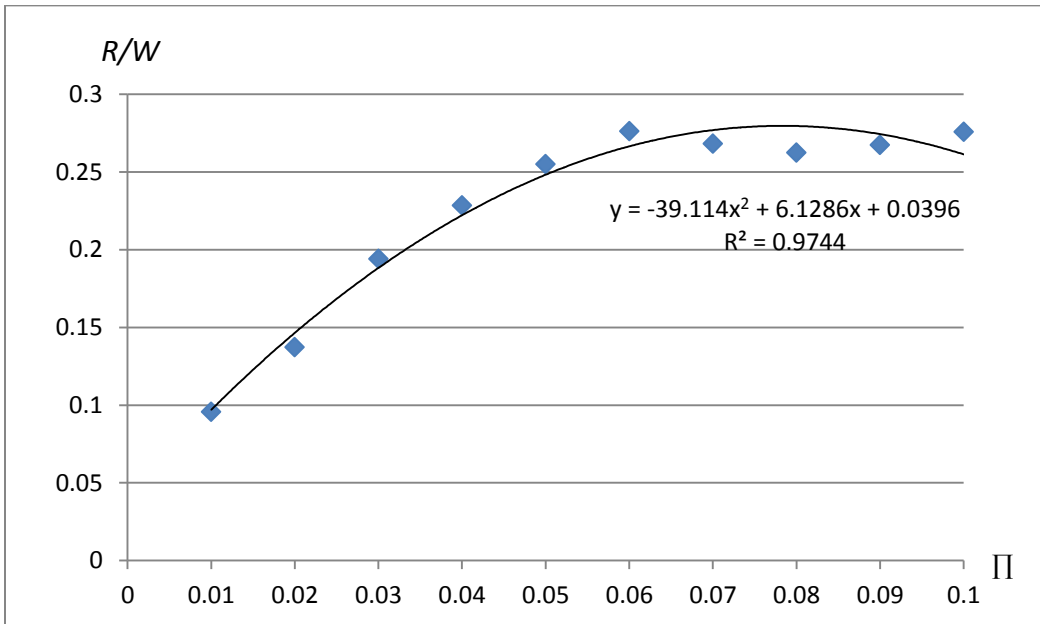


Figure 3-16. Relations of R/W and π of the fixed toll pricing strategy

For the linear pricing strategies, we compared our results with analytical equations as in the previous $\frac{W_1(a)}{W}$ analysis. Converting (18e) into linear equation in terms of a gives us :

$$\frac{R(a)}{W} = a\bar{\mu}_1 = ac_1 + c_0. \quad (31)$$

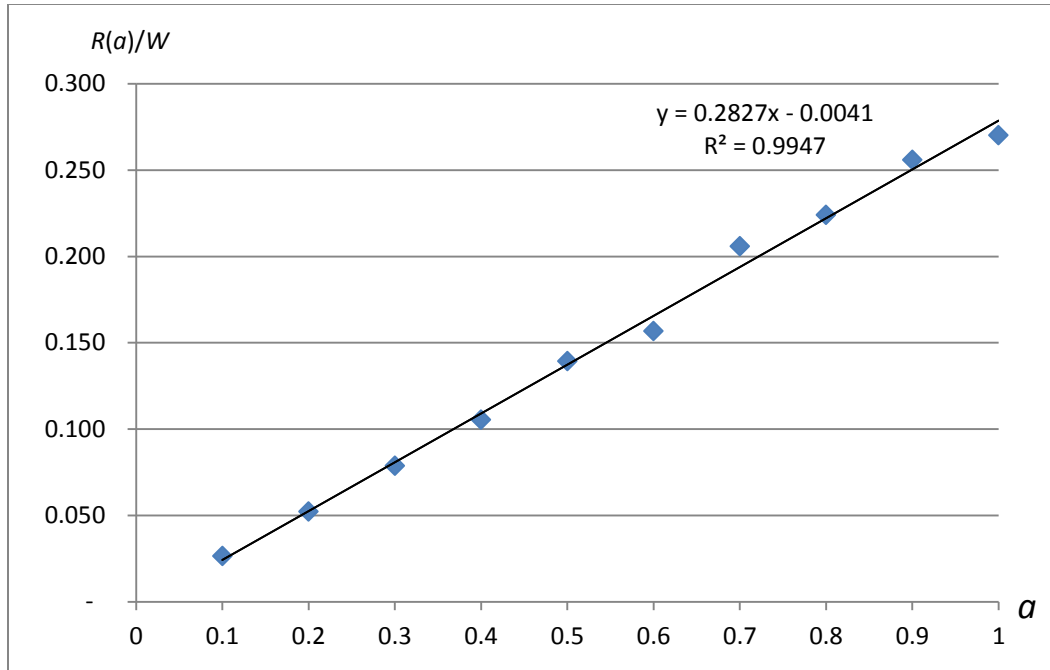
Repeatedly, average $\bar{\mu}_1$ of all cases in CLT and VLT were 0.2718 and 0.2743 respectively. After substituting these numbers into (31), and obtaining coefficients of linear regression equations of simulation data as Figure 3-17(a) and (b), we compared 95% confidence intervals of coefficients; see Table 3-4.

Table 3-4. Comparing equation (31) and simulation results

		c_1	c_0
CLT	eq.(31)	(0.2603, 0.2789)	-
	Simulation	(0.2658, 0.2996)	(-0.0146, 0.0064)
VLT	eq.(31)	(0.2697, 0.2789)	-
	Simulation	(0.2723, 0.2972)	(-0.0153, 0.0001)

As in the $\frac{W_1(a)}{W}$ analysis, it was noticeable that our simulation results were very close to the analytical expressions.

(a) CLT



(b) VLT

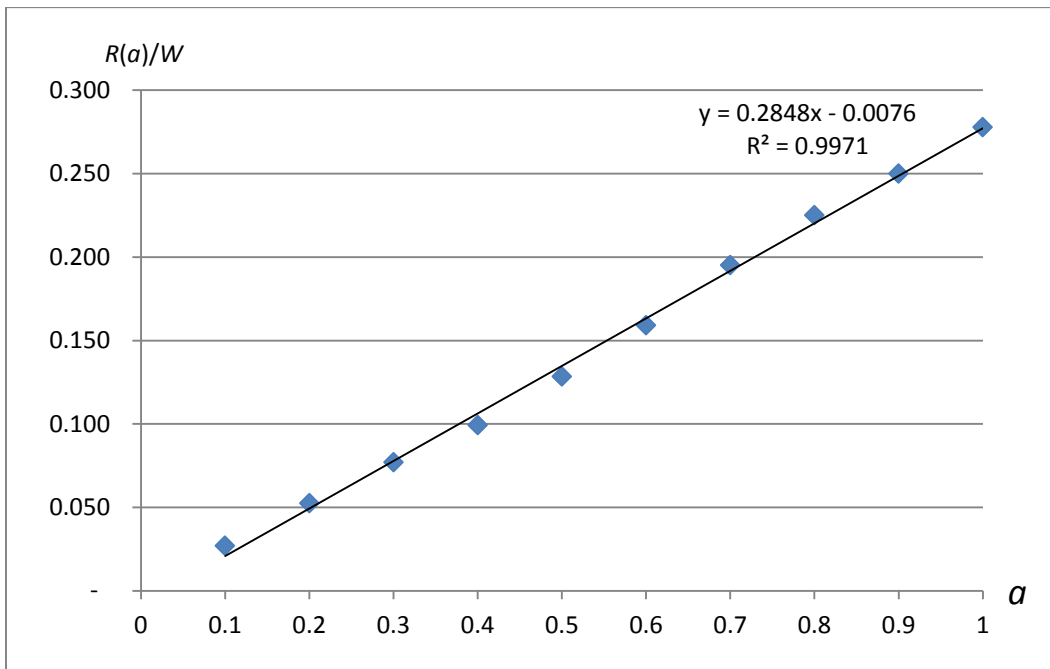


Figure 3-17. Relations of $R(a)/W$ and a in (a) CLT and (b) VLT

Table 3-3 and 3-4 shows that our simulation experiments closely approximate to analytical models. We compared measures of effectiveness (MoE) of pricing strategies; see Table 3-5. We found that from a social cost point of view, VLT is the most efficient pricing strategy among the three. However, in VLT, delay of HOT lane was larger than FT that VLT toll-paid users would have less benefit (i.e. saving travel time) than FT toll-paid users. From an operator's perspective, revenue of FT was the highest that FT would be the optimal solution for them. Finally, comparing CLT and VLT, only small amounts of differences in performances were detected.

Table 3-5. Performance comparison of pricing strategies' MoE.

MoE		FT	CLT	VLT
Delay	W	●	◐	◑
	W_0	●	◐	◑
	W_1	○	◐	◑
Revenue	R	●	◑	◑

(Magnitudes of MoE: ○ < ◐ < ◑ < ●)

Additionally, we presented samples of input-output diagrams, oblique input-output diagrams, departure rates, and $\bar{\mu}_0, \bar{\mu}_1$ by time for each pricing strategy, i.e. $\pi = 0.06 \text{ hr}$ for FT, and $a=0.8$ for CLT and VLT. See Figure 3-18-21.

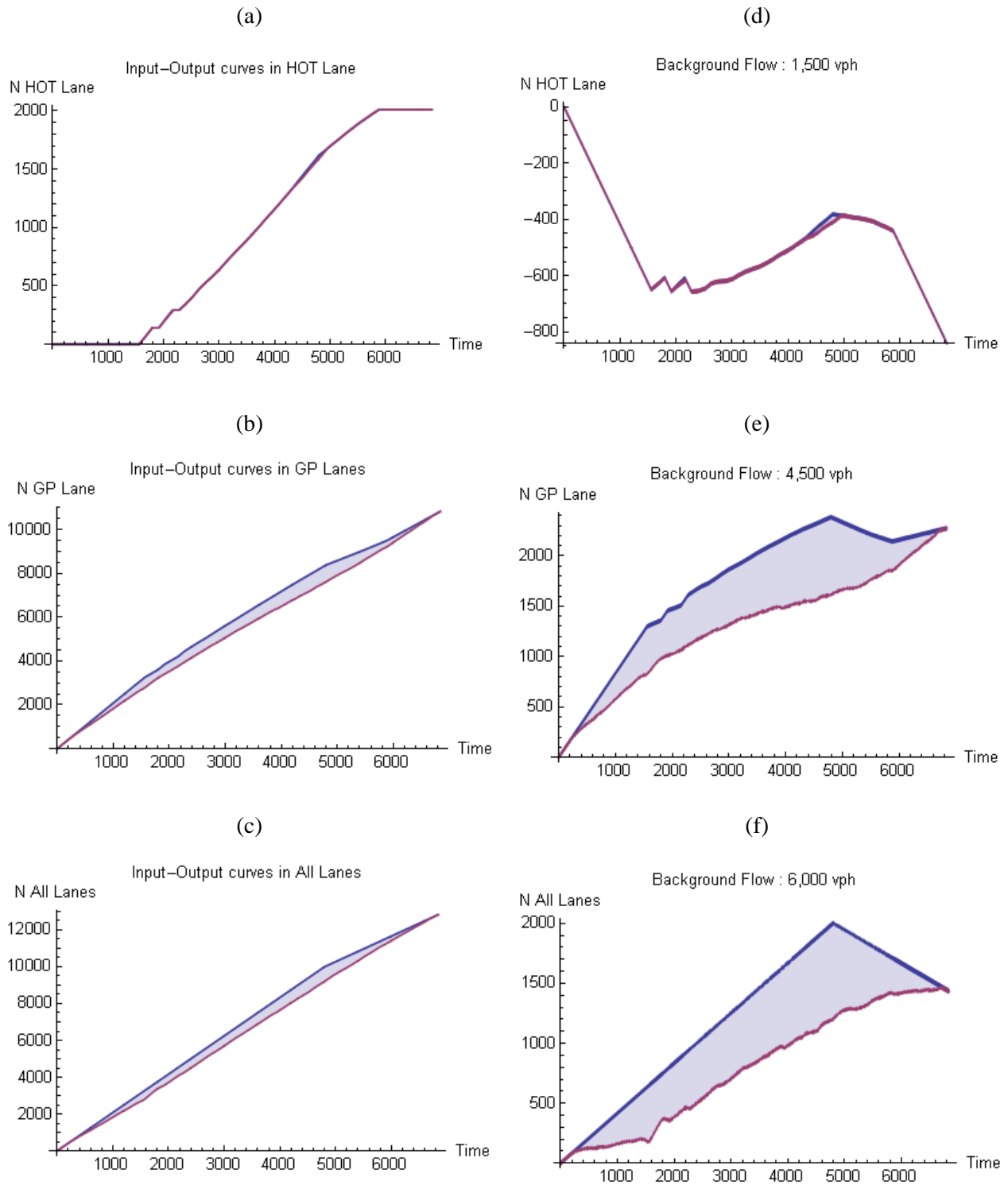


Figure 3-18. Fixed toll pricing strategy's ($\pi=0.06$ hr) (a) Input-output diagram for HOT lane; (b) GP lanes; (c) All lanes; (d) Oblique input-output diagram for HOT lane; (e) GP lanes; (f) All lanes

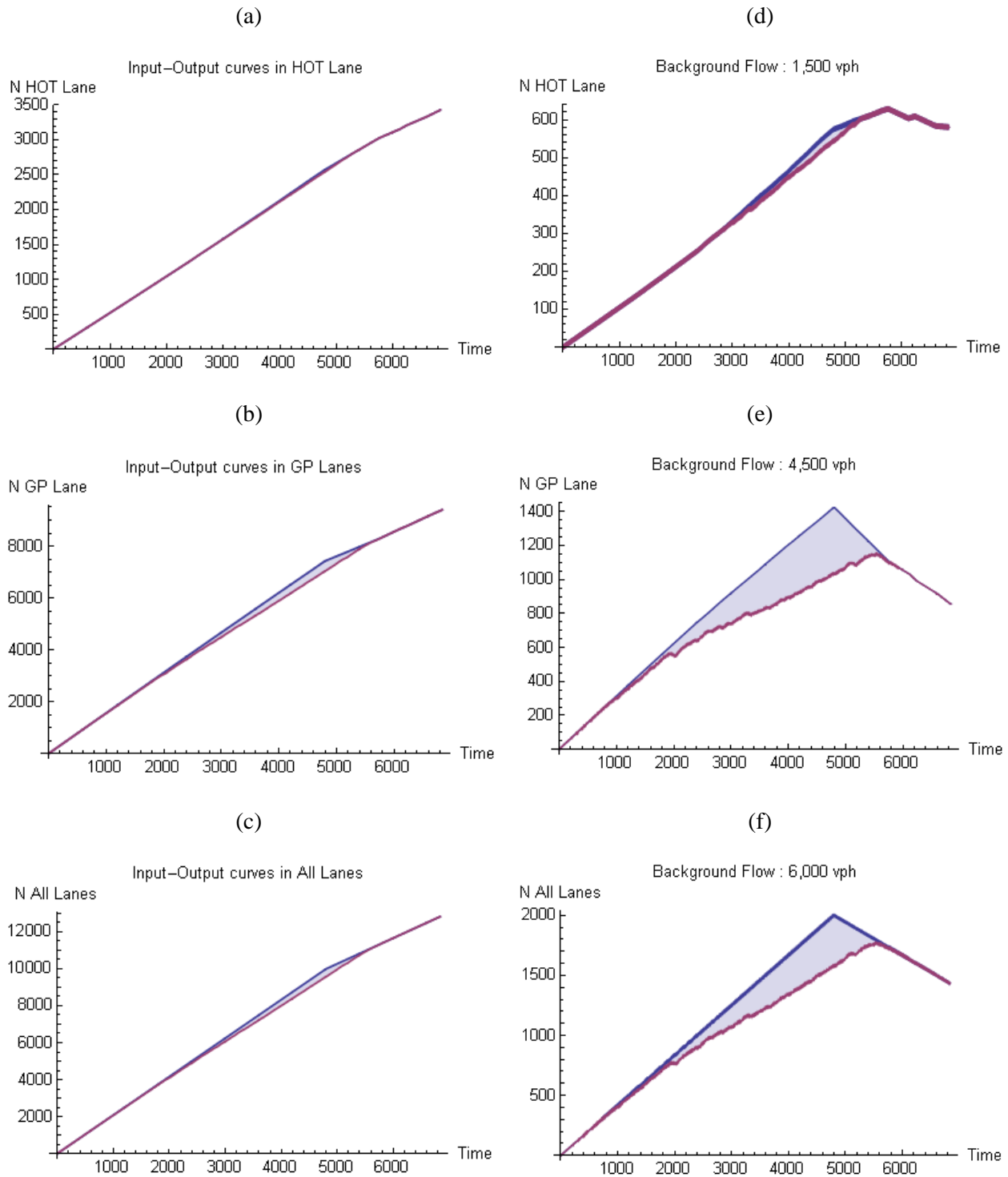


Figure 3-19. Constant bottleneck capacity Linear Toll Pricing Strategy's ($a=0.8$) (a) Input-output diagram for HOT lane; (b) GP lanes; (c) All lanes; (d) Oblique input-output diagram for HOT lane; (e) GP lanes; (f) All lanes.

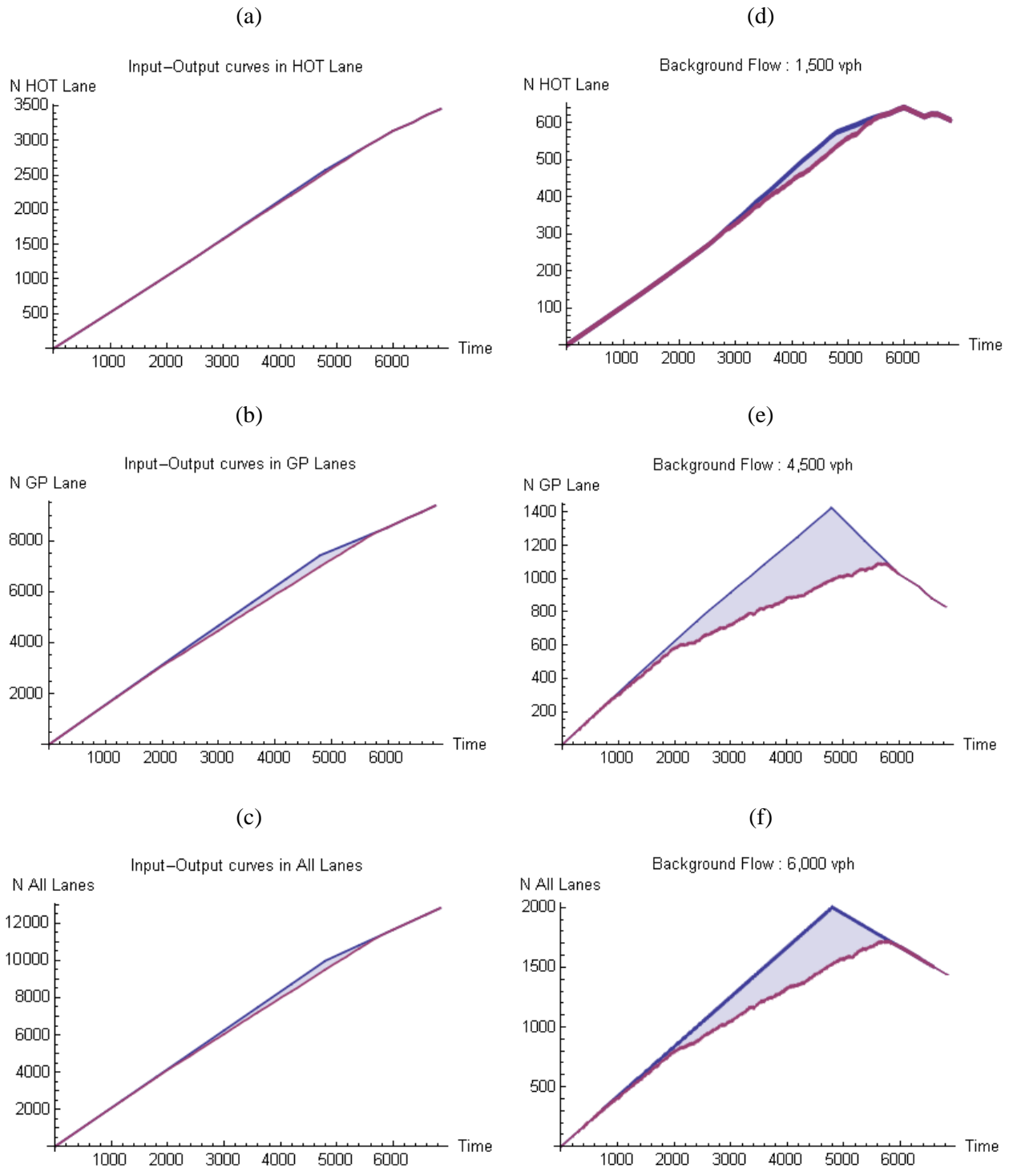


Figure 3-20. Variable bottleneck capacity Linear Toll Pricing Strategy's ($\alpha=0.8$) (a) Input-output diagram for HOT lane; (b) GP lanes; (c) All lanes; (d) Oblique input-output diagram for HOT lane; (e) GP lanes; (f) All lanes.

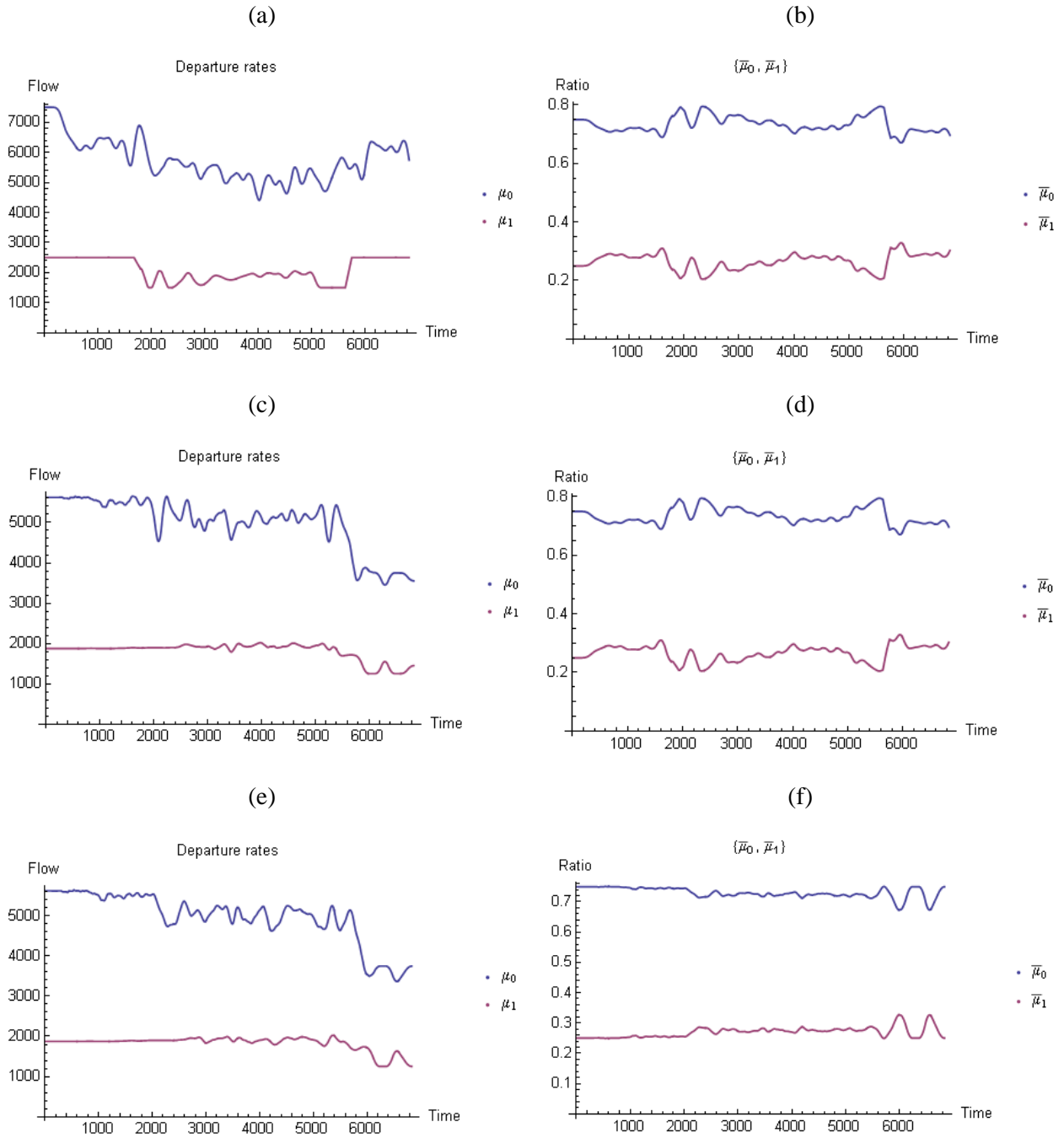


Figure 3-21. (a) Departure rates and (b) $\bar{\mu}_0, \bar{\mu}_1$ of the fixed toll pricing strategy's ($\pi=0.06$ hr); (c) Departure rates and (d) $\bar{\mu}_0, \bar{\mu}_1$ of the CLT's ($a=0.8$); (e) Departure rates and (f) $\bar{\mu}_0, \bar{\mu}_1$ of the VLT's ($a=0.8$)

CHAPTER 4 DYNAMIC PRICING FOR HIGH-OCCUPANCY/TOLL LANES WITH REFUND OPTION

INTRODUCTION

Operation strategies of managed lanes (ML) often employ a combination of vehicle eligibility and road pricing to manage the demand and to improve the traffic conditions of the facility. While MLs aim to provide an alternative travel choice for road users, travellers, in general, may have a negative attitude towards pricing of MLs (Ungemah et al. (2005)). One plausible reason is that paid ML users may not receive the benefits they expected due to uncertainties in traffic. This has created a growing challenge of developing innovative pricing strategies to support ML goals that range from operational efficiency to social benefits as well as public acceptance.

In order to improve travelers' experiences with MLs and boost the public acceptance (and thus the feasibility) of ML pricing, this chapter explored an innovative solution by introducing a refund option. When choosing to pay to gain access to MLs, a traveler was offered the chance to purchase an additional refund option. Part (or all) of the toll paid by the traveler was refunded if the travel time saving did not reach some minimal amount guaranteed by the operator. The goal of this pricing scheme was to achieve the operational objectives of MLs such as desired facility level of service and revenue return that can cover refund claims, and at the same time make MLs appeal more to the travelers.

With the premise that appropriate advanced technologies, such as Connected Vehicle (Research and Innovative Technology Administration, 2014) applications, are in place for ML operators to obtain actual travel time of each individual vehicle, this study investigated

approaches to determining optimal operational parameters for the proposed ML pricing scheme with a refund option. The operational parameters included the toll rate π , the refund amount r , the premium for the refund option f , the travel time saving guaranteed by the operator $\bar{\tau}$.

METHODOLOGIES

Similar to the author's previous research (Lou (2013), Lou et al. (2011), Yin and Lou (2009)), this study considered dynamic pricing for High/Occupancy Toll (HOT) lanes. HOT lanes are a prevalent form of priced MLs in the US; and to achieve the operational objectives of HOT lanes, ideally the toll rate should be adjusted dynamically in response to real-time traffic condition as well as travelers' willingness to pay (WTP). The success of such operation depends on accurate prediction of travelers' lane choices and estimation of traffic conditions along the facility, as well as carefully designed toll rates. Lou (2013) has proposed a proactive self-learning framework that consists of two critical steps: system inference and toll optimization. Through mining real-time traffic data (such as speed, flow or occupancy) collected at a regular time interval from loop detectors (often at limited locations), the first step learns travellers' WTP and predicts their lane choices when facing the tolls based on certain lane choice models, delivers a full picture of current traffic condition of the entire facility using certain traffic flow models, and forecasts short-term traffic demand by employing statistical modelling. The attained knowledge up to the current time point is then used in the second step to determine the optimal toll rate for the next tolling interval in order to achieve the operational objectives of HOT lanes.

The focus of this chapter was the determination of the operational parameters for the proposed dynamic pricing scheme with a refund option. The system inference component in the framework (Lou (2013)), therefore, was not considered. Instead, simple models were employed

for travelers' lane choices and traffic propagation to allow more in-depth analysis of the proposed innovative pricing scheme.

LANE CHOICE MODEL

It was assumed that each traveler follows a set of deterministic utility functions with her own WTP parameters, and the WTP parameters followed a certain distribution across the population. The following deterministic utility functions were assumed for each individual vehicle not qualified for free access to the HOT lane. U_1' represents the utility of choosing to pay for HOT lane access with the purchase of the refund option; U_1 the utility of paying for HOT lane access without purchasing the refund option; and U_0 the utility of choosing to continue on the general purpose lane.

$$U_1' = -\hat{t}_1 - v(\pi + f) + vr \cdot \Pr(\tau_0 - \tau_1 < \bar{\tau})$$

$$U_1 = -\hat{t}_1 - v\pi$$

$$U_0 = -\hat{t}_0$$

In the above, v represents a traveler's WTP, which is essentially the inverse of the traveler's value of time (VOT); τ_0 and τ_1 are the travel times (random due to intrinsic uncertainties in traffic) for the general purpose and the HOT lanes respectively; and \hat{t}_0 and \hat{t}_1 are the expected travel times. Note it was assumed that \hat{t}_0 , \hat{t}_1 , as well as $\Pr(\tau_0 - \tau_1 < \bar{\tau})$ were provided to the traveller by the operator when the traveller approaches the HOT facility from the general purpose lane. They were not necessarily related to the actual travel experience of this traveller.

From the utility functions, the followings were derived.

- Choosing 0 (General purpose lane) implies $(U_1 > U_{1'})$ and $(U_0 > U_1)$

$$\Rightarrow v > \frac{\hat{\tau}_0 - \hat{\tau}_1}{\pi + f - r \cdot \Pr(\tau_0 - \tau_1 < \bar{\tau})} \quad \text{and} \quad v > \frac{\hat{\tau}_0 - \hat{\tau}_1}{\pi}$$

- Choosing I (HOT lane without refund) implies $(U_1 > U_0)$ and $(U_1 > U_{1'})$

$$\Rightarrow f - r \cdot \Pr(\tau_0 - \tau_1 < \bar{\tau}) > 0 \quad \text{and} \quad v < \frac{\hat{\tau}_0 - \hat{\tau}_1}{\pi}$$

- Choosing I' (HOT lane with refund) implies $(U_{1'} > U_0)$ and $(U_{1'} > U_1)$

$$\Rightarrow v < \frac{\hat{\tau}_0 - \hat{\tau}_1}{\pi + f - r \cdot \Pr(\tau_0 - \tau_1 < \bar{\tau})} \quad \text{and} \quad f - r \cdot \Pr(\tau_0 - \tau_1 < \bar{\tau}) < 0$$

To simplify the notation, the following was introduced.

$$A := \frac{\hat{\tau}_0 - \hat{\tau}_1}{\pi}$$

$$B := \frac{\hat{\tau}_0 - \hat{\tau}_1}{\pi + f - r \cdot \Pr(\tau_0 - \tau_1 < \bar{\tau})}$$

It was worth mentioning that the expected net cost of the refund option, $f - r \cdot \Pr(\tau_0 - \tau_1 < \bar{\tau})$, was a critical value in a user's lane choice. In fact, if the expected net cost is positive, all the travellers with $v > A$ choose 0 ; and all the travellers with $v < A$ choose I . On the other hand, if the net cost is negative, all travelers with $v > B$ choose 0 ; and all travelers with $v < B$ choose I' .

TRAFFIC MODEL

To account for the intrinsic uncertainty in traffic flow, this study adopted a modified point queue model. Suppose a vehicle enters the facility at a time point where x vehicles are in the downstream vertical queue and y vehicles are on the link but have not joined the queue yet. Then the travel time of this vehicle, denoted as $c(x, y)$, is a function of the free-flow travel time c_0 , both x and y , and the discharge process at the downstream bottleneck. The discharge process is stochastic, where the discharge headways were assumed to follow independent and identical normal distributions with a mean of the saturation discharge headway \bar{h} and a variance of σ^2 , if the downstream bottleneck is oversaturated. Otherwise, the vehicle's travel time was simply the free-flow travel time if no queue was present when it reached the downstream end of the facility. Based on the above discussion, $c(x, y)$ is further approximated by a normal distribution with mean $\hat{c}(x, y)$ and variance $\tilde{c}^2(x, y)$, where

$$\begin{aligned}\hat{c}(x, y) &= c_0 + \max\left\{x + y - \frac{c_0}{\bar{h}}, 0\right\} \cdot \bar{h} \\ \tilde{c}(x, y) &= \max\left\{x + y - \frac{c_0}{\bar{h}}, 0\right\} \cdot \sigma\end{aligned}\tag{1}$$

DYNAMIC PRICING WITH REFUND OPTION

The primary operational objective of HOT lanes was to make full use of its available capacity while maintaining free-flow traffic condition. To this end, a chance constraint was employed to determine the desired inflow to the HOT facility during tolling interval k . Suppose the number of high occupancy vehicles (those qualified for free access) arriving the upstream end of the facility during interval k is θ_1^k , and the number of lower occupancy vehicles is θ_0^k .

Inflows to the facility up to interval k were denoted as λ_1^l and λ_0^l for all $l < k$. The vertical queues at the downstream bottleneck of the facility at the beginning of tolling interval k were denoted as q_1^{k-1} and q_0^{k-1} respectively. Further assume t_0 was m (integer) times of a tolling interval Δt . The desired inflows $\tilde{\lambda}_1^k$ and $\tilde{\lambda}_0^k$ are determined by the following optimization problem.

$$\begin{aligned}
& \max \tilde{\lambda}_1^k \\
& s.t. \quad \Pr\left(c_1\left(q_1^{k-1}, \sum_{i=1}^m \lambda_1^{k-i} + \tilde{\lambda}_1^k\right) \leq (m+1)\Delta t\right) \geq p \\
& \quad \tilde{\lambda}_1^k + \tilde{\lambda}_0^k = \theta_1^k + \theta_0^k \\
& \quad \tilde{\lambda}_1^k \text{ and } \tilde{\lambda}_0^k \text{ are integers}
\end{aligned} \tag{2}$$

Essentially, the optimization model seeks to prompt as many travelers as possible to use the HOT lane, as long as the last user entering the HOT lane during interval k has a minimum chance of p to experience free-flow travel. The solution to the above model is analytically derived as

$$\tilde{\lambda}_1^k = \left\lfloor \frac{\Delta t}{\sigma \Phi_N^{-1}(p) + \bar{h}_1} - \frac{1}{\bar{h}_1} \cdot \hat{c}\left(q_1^{k-1}, \sum_{i=1}^m \lambda_1^{k-i}\right) \right\rfloor \tag{3}$$

where Φ_N^{-1} is the inverse cumulative distribution function of the standard normal random variable, and \bar{h}_1 the average saturation discharge headway for the HOT lane.

If $\theta_1^k < \tilde{\lambda}_1^k < \theta_1^k + \theta_0^k$, pricing should be implemented to achieve $\tilde{\lambda}_1^k$. To this end, the operator needs to determine the toll rate π^k , the refund amount r^k , the premium for the refund option f^k , and the guaranteed travel time saving $\bar{\tau}^k$ for tolling interval k . In addition, the operator also needs to provide $\hat{\tau}_0^k, \hat{\tau}_1^k$, as well as $\Pr(\tau_0^k - \tau_1^k < \bar{\tau}^k)$, to all the travellers

approaching the facility during tolling interval k . Since the focus of this study was on operational parameters, the operator-provided traffic information was set as

$$\begin{aligned}\hat{\tau}_1^k &= \hat{c}_1 \left(q_1^{k-1}, \sum_{i=1}^m \lambda_1^{k-i} + \tilde{\lambda}_1^k \right) \\ \hat{\tau}_0^k &= \hat{c}_0 \left(q_0^{k-1}, \sum_{i=1}^m \lambda_0^{k-i} + \tilde{\lambda}_0^k \right)\end{aligned}\tag{4}$$

Note that $\hat{\tau}_1^k$ and $\hat{\tau}_0^k$ represent the predicted expected travel times of the last traveller entering each lane during tolling interval k , if the inflows to the HOT and the general purpose lanes are exactly $\tilde{\lambda}_1^k$ and $\tilde{\lambda}_0^k$.

Without loss of generality, the superscription k was dropped for simplicity of the notation.

Based on the discussion in Lane Choice Model Section, this study investigated the cases where $f - r \cdot \Pr(\tau_0 - \tau_1 < \bar{\tau}) > 0$ and $f - r \cdot \Pr(\tau_0 - \tau_1 < \bar{\tau}) < 0$ separately.

Paradigm 1: Positive net expected cost of the refund option

In this case, the operator set the values of f , r , and $\Pr(\tau_0 - \tau_1 < \bar{\tau})$ such that $f - r \cdot \Pr(\tau_0 - \tau_1 < \bar{\tau}) > 0$. The problem was reduced to determining the value of τ such that $\Phi_v^{-1}(A) = \tilde{\lambda}_1$, where $\Phi_v^{-1}(\cdot)$ is the inverse cumulative distribution of v . Note that since $v = 1/\text{VOT}$, $\Phi_v^{-1}(x) = 1/\Phi_{\text{VOT}}^{-1}(1 - x)$, where $\Phi_{\text{VOT}}^{-1}(\cdot)$ is the inverse cumulative distribution of VOT. The analytical solution to this problem was

$$\tau = \frac{\hat{t}_0 - \hat{t}_1}{\Phi_v^{-1}\left(\frac{\tilde{\lambda}_1 - \theta_1}{\theta_0}\right)}\tag{5}$$

Paradigm 2: Negative net expected cost of the refund option

In this case, the operator set the values of π , f , r , and $\Pr(\tau_0 - \tau_1 < \bar{\tau})$ such that

$$f - r \cdot \Pr(\tau_0 - \tau_1 < \bar{\tau}) < 0 \quad \text{and} \quad \Phi_v^{-1}(B) = \tilde{\lambda}_1.$$

There are four decision parameters and only two equations. Therefore, this system was underdetermined, and multiple solutions existed.

Note that in both paradigms, the determination of f , r , and $\Pr(\tau_0 - \tau_1 < \bar{\tau})$ should have the financial feasibility of the operation as one of the considerations.

SIMULATION AND PRELIMINARY RESULTS

A simulation framework similar to the author's previous research (Lou et al. (2011)) was adopted to investigate the approach under Paradigm 1. The only difference here was that a Monte Carlo approach was implemented to simulate the randomness in lane choice (due to VOT distribution) and traffic propagation (due to random discharge headway).

The framework consists of three major components:

- A controller that implements equations (3) – (5) to calculate the desired inflows to the HOT and the general purpose lanes during tolling interval k ($\tilde{\lambda}_1^k$ and $\tilde{\lambda}_0^k$), the predicted expected travel times of the last traveller entering each lane ($\hat{\tau}_1^k$ and $\hat{\tau}_0^k$), and the optimal toll rate π ;
- A lane-choice simulator that generates random numbers according to the assumed VOT distribution to simulate each traveler's lane choice;

- A traffic simulator that generates random travel time for each traveler according to equation (1).

Note that pricing should only be implemented when $\theta_1^k < \tilde{\lambda}_1^k < \theta_1^k + \theta_0^k$. When $\tilde{\lambda}_1^k \leq \theta_1^k$, the demand of HOVs is high enough to warrant an exclusive HOV lane, and no lower occupancy vehicles are allowed to enter the HOV/HOT lane. When $\tilde{\lambda}_1^k \geq \theta_1^k + \theta_0^k$, the demand is low enough to open the HOT lane for general use. In this case, the toll rate is 0; and the inflows are assumed proportional to the remaining capacity:

$$\lambda_1^k = \theta_1^k + \theta_0^k \cdot \frac{\mu_1 - \theta_0^k}{\mu_1 + \mu_0 - \theta_0^k} \quad (6)$$

where μ_1 and μ_0 are the saturation flow rates at the downstream bottleneck.

Note that in Paradigm 1, as long as the operator sets the values of f , r , and $\Pr(\tau_0 - \tau_1 < \bar{\tau})$ such that $f - r \cdot \Pr(\tau_0 - \tau_1 < \bar{\tau}) > 0$, the critical VOT value that governs the choice between general purpose and HOT lanes (and thus the traffic condition) only depends on π . Therefore, the experiments were focused on determining the toll rate π only. The financial feasibility of the operation (determination of f , r , and $\Pr(\tau_0 - \tau_1 < \bar{\tau})$) was not considered in the experiments.

Simulation Settings

Figure 4-1 illustrates the simulated HOT facility. It has one HOV/HOT lane and one general purpose lane. In order to create congested traffic condition, it was assumed that a downstream bottleneck was active. The free flow travel time for the simulated freeway segment was set as four times the tolling interval ($m = 4$), i.e., 8 minutes. If the free flow speed is 60

mph, the facility is 8 miles long. The average saturation flow rates at the downstream bottleneck (μ_1 and μ_0) were set to 1800 vph and 2400 vph for the HOT and the general purpose lanes respectively. This is equivalent to setting $\bar{h}_1 = 2$ seconds and $\bar{h}_0 = 1.5$ seconds. The standard deviation of the saturation headway was set as 10% of the mean, for both HOT and general purpose lanes. The upstream saturation flows were set to 1800 vph and 3600 vph respectively.

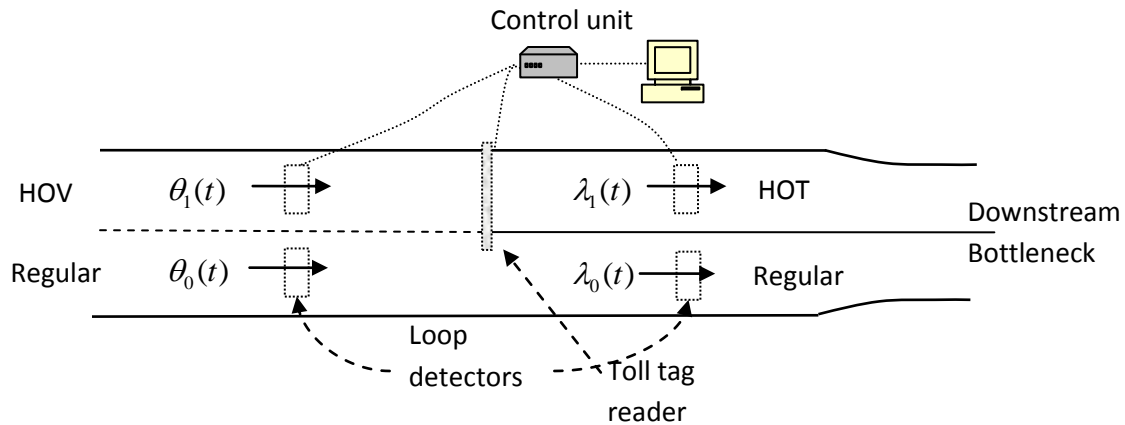


Figure 4-1. Simulated HOT lane facility

The dynamic tolling interval Δt was set to 2 minutes. A total of 44 time intervals (88 minutes) was simulated. The upstream inflow rate for the HOT lane θ_1^k was set to exactly 10 vehicles per time interval (equivalent to 300 vph) throughout the simulation duration. For the general purpose lane, the upstream inflow rate θ_0^k was set to exactly 120 vehicles per time interval (equivalent to 3600 vph) for the first 24 time intervals (48 minutes), and 60 vehicles per interval (equivalent to 1800 vph) for the last 20 time intervals (40 minutes). The first 4 time intervals (8 minutes) of the entire simulation duration were warm-up periods, where the HOT

lane was not activated. Therefore, the inflows λ_1^k and λ_0^k were 10 vehicles and 120 vehicles for every interval during the initial 4 intervals.

Similar to Gardner et al. (2013), a Burr function was adopted for VOT distribution with two parameters ξ and γ .

$$\Phi_{\text{VOT}}(x) = \Pr(\text{VOT} \leq x) = 1 - \frac{1}{1 + \left(\frac{x}{\xi}\right)^\gamma}$$

Therefore,

$$\Phi_v^{-1}(x) = \frac{1}{\Phi_{\text{VOT}}^{-1}(1-x)} = \frac{1}{\xi} \cdot \left(\frac{1-x}{x}\right)^\gamma$$

ξ represents the median VOT, and γ is a shape parameter. In this simulation, ξ was set to 15 (\$/hr), and γ was set to 2.

Results

Two experiments were performed for Paradigm 1 with different target p values (the probability for the last user entering the HOT lane during a tolling interval to experience free-flow travel).

For each experiment, ten simulation replications were performed. The inflows, queue lengths, and toll rates were recorded for both lanes at each time interval. The results are presented below.

Experiment 1: $p = 0.85$.

The performance of the facility from the first simulation replication of this experiment (Exp. 1, Run 1) is shown in Figure 4-2. The corresponding toll rate is shown in Figure 4-3.

During the warm-up period (first 8 minutes), the HOV/HOT lane operates as an HOV-only lane. The toll rates were zeros during these time period. The inflows to HOT and general purpose lanes (λ_1^k and λ_0^k) were constant and equal to the upstream inflows (θ_1^k and θ_0^k). Since it took 4 time intervals (8 minutes) in free flow for a vehicle to arrive at the downstream bottleneck, the queue started to build up starting at the 8th minute for the general purpose lane. At the same time, the HOV/HOT lane started to open to lower occupancy vehicles with a toll. The toll rates (Figure 4-3) vary between \$1 and \$1.5 from time interval 5 to 24 (minute 8 to 48) when the demand is higher. After the upstream arrival rate dropped at minute 48, the facility kept operating as an HOT lane for another two time intervals with significantly lower rates (Figure 4-3). When the toll rate completely dropped to zero after minute 52 and both lanes were open to all traffic, the inflows to both lanes became stable, proportional to available capacities (see equation (6)).

Note that the downstream discharge headway was considered a random variable in order to model the uncertainty in travel time. Although the downstream saturation flow rate was 60 vehicles per time interval, the desired HOT inflow was lower than 60 to satisfy the chance constraint (2). For this simulation replication, the desired inflow to HOT lane was calculated as 54 vehicles per interval from equation (3); and it is seen from Figure 4-2 that the actual inflow to HOT lane varies around the desired value due to random VOT of the approaching vehicles.

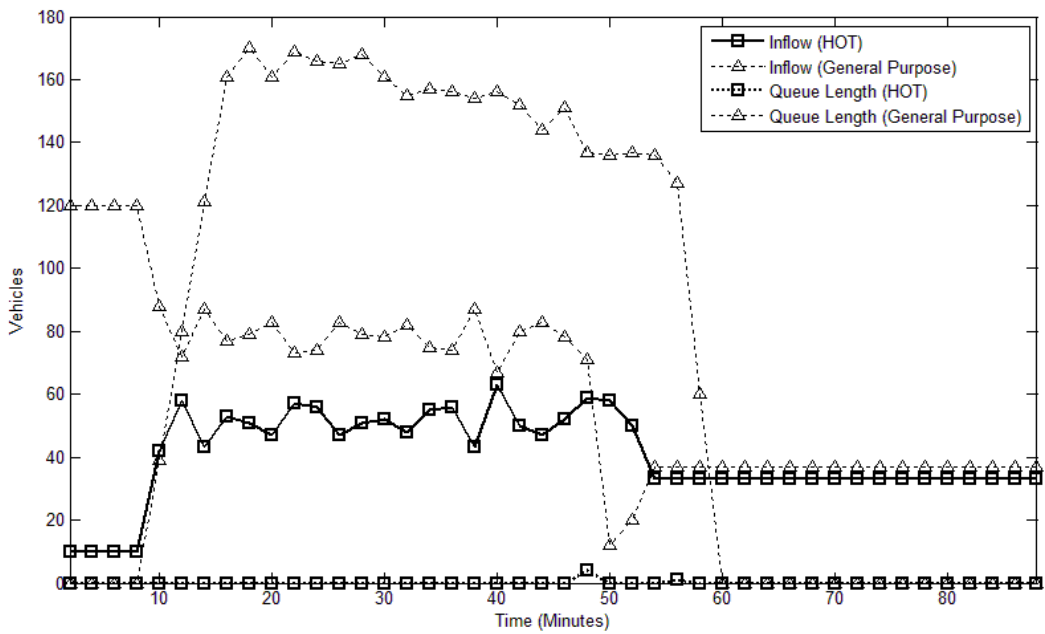


Figure 4-2. Facility performance (Exp. 1, Run 1)

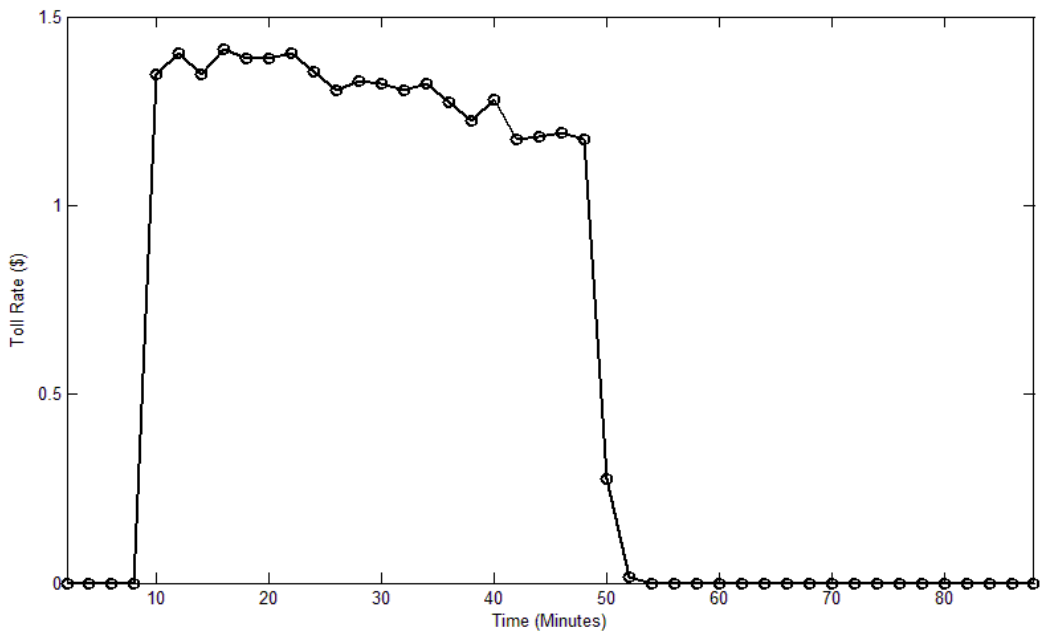


Figure 4-3. Toll rates (Exp. 1, Run 1)

The inflow to HOT lane during interval 5 to interval 26 (minute 8 to minute 52) when the facility was active ranges from 43 to 63 vehicles per time interval, with an average value of 51.73. This value was lower than the calculated desired value of 54 vehicles per interval. Therefore, it was no surprise that there was no queue on the HOT lane for the most part of the simulation duration (see Figure 4-2). In fact, there were only two-time intervals where the queue was present on the HOT lane. At the end of interval 24 (minute 48), the HOT lane had a 4-vehicle queue. This corresponded well with the highest inflow observed for the HOT lane during interval 20 (minute 38 to 40, see Figure 4-2). At the end of interval 28 (minute 56), the HOT lane had a 1-vehicle queue. This was because that the HOT lane was still active with a relatively high inflow during intervals 25 and 26 (minute 48 to 52), and it was still possible to form queues due to the random discharge headway at the downstream bottleneck.

On the other hand, although the inflows to general purpose lane were significantly reduced when the HOT lane was active, the general purpose lane was still severely congested because the total demand was much higher than the total capacity at the downstream bottleneck. When the total demand dropped at the beginning of interval 25 (minute 49), the HOT lane was still in effect but with significantly lower toll rates, prompting a large percentage of travelers to use HOT lane. This led to a substantial drop of inflow to the general purpose lane during interval 25 and 26 (minute 48 to 52). It is seen from Figure 4-2 that the inflow to the general purpose lane during these 4 minutes is significantly lower than that to the HOT lane. This prevented the existing queue on the general purpose lane from growing and helped it to dissipate. No new queue was formed after the existing queue was discharged since the new demand and inflow was much less than the downstream capacity.

Two performance measures are of interest: the maximum queue length and the percentage time when the queue was present for the HOT lane. The latter was related to the chance constraint (2) and represented the probability for the last user entering the HOT lane during a tolling interval to encounter a queue. Suppose the HOT lane is active starting at interval k_1 and ending at interval k_2 . Because the free-flow travel time is m time intervals, this metric should be calculated as the number of intervals when queue is present between intervals $k_1 + m$ and $k_2 + m$ divided by $(k_2 - k_1 + 1)$. Any HOT queue presented after interval $k_2 + m$ was not related to the p value in chance constraint (2). However, it indicated a failure in HOT operation, as too many vehicles opted in the facility and created additional congestion. For Exp. 1, Run 1, the HOT lane was active between intervals 5 and 26 (minute 8 to 52 for a total of 44 minutes), and no queue was present after interval 30. The percentage time when queue was presented for the HOT lane was $2/22 = 9.09\%$, which was lower than the target value of $1 - p = 1 - 0.85 = 15\%$. The maximum HOT queue length is 4.

Results from another simulation replication (Exp. 1, Run 2) are presented in Figure 4-4 and Figure 4-5. It was observed that the general trends of the inflows, the queue lengths, and the toll rates were similar to the results of Exp. 1, Run 1. The toll rates (Figure 4-5) are a little lower comparing to the previous replication, varying between \$0.7 and \$1.35 when the demand is higher. The facility keeps operating as an HOT lane for only one additional time interval with a toll rate of \$0.08 after the upstream arrival rate drops at minute 48. The inflow to HOT lane ranged from 41 to 66 vehicles per time interval with an average value of 54.14, when HOT facility is active. The average is very close to the target inflow of 54 vehicles per time interval. However, due to a series of relatively high HOT inflows during intervals 21 to 25 (minute 40 to 50), queue is present on the HOT lane during intervals 25 to 27 (minute 48 to 54). A fourth

interval when the queue is present on the HOT lane is interval 17. No queue is present after interval $25 + 4 = 29$ (minute 58). The percent time when the queue is present for or the HOT lane is $4/21 = 19.05\%$, higher than the target value of 15%. The maximum HOT queue length is 9.

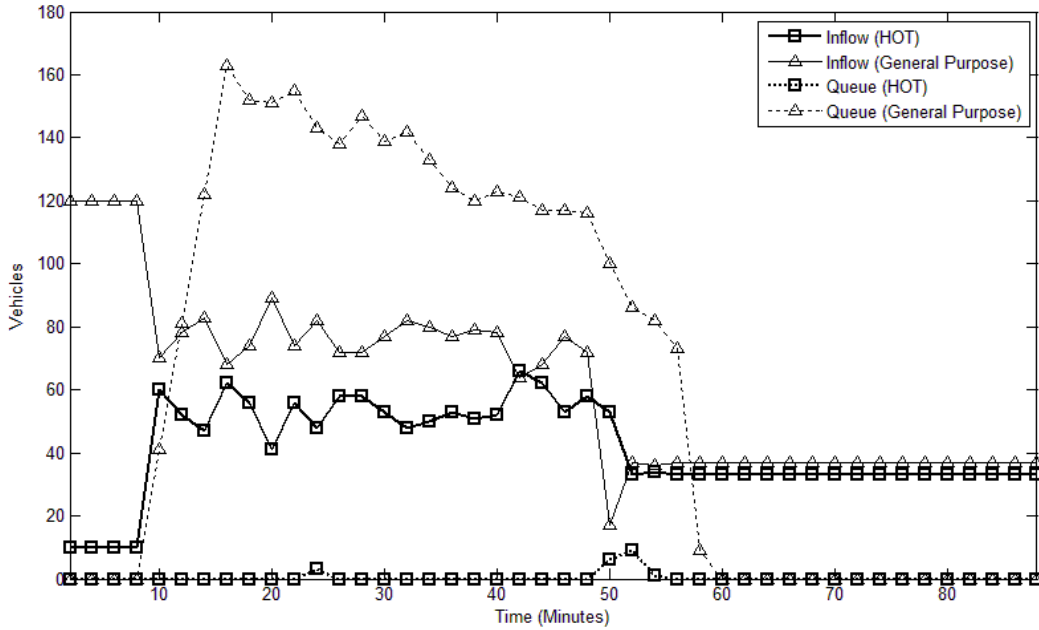


Figure 4-4. Facility performance (Exp. 1, Run 2)

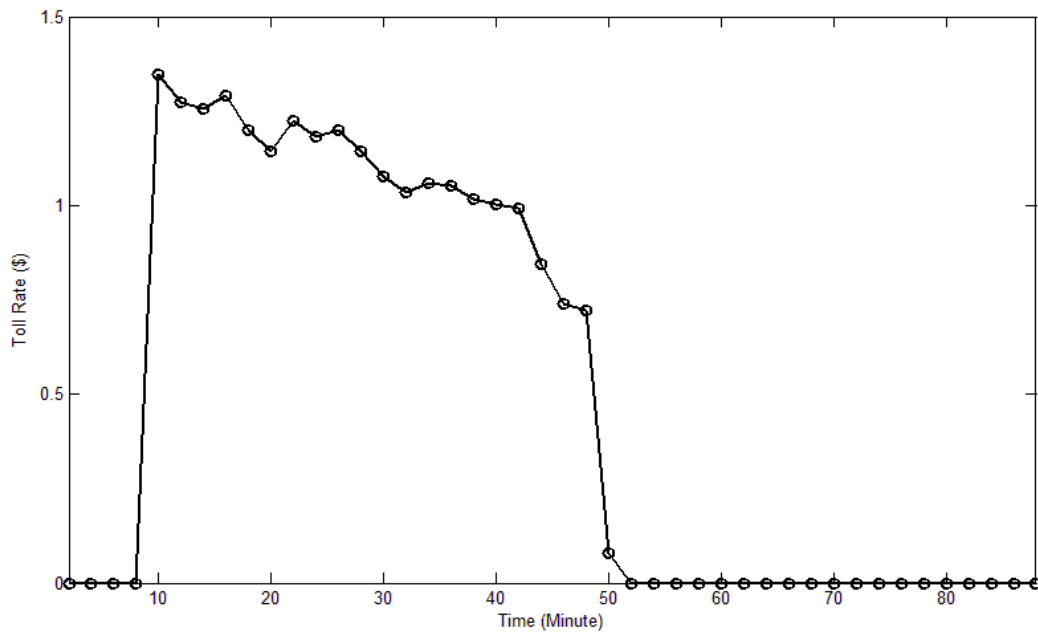


Figure 4-5. Toll rates (Exp. 1, Run 2)

Across the 10 simulation replications, the maximum HOT queue length varies from 1 to 9 vehicles, with an average value of 4.30. No queue was present beyond 4-time intervals after the last tolling interval. The average percentage time when the queue was present for the HOT lane was 16.43%, slightly higher than the operational goal of 15%. The toll rate ranged from \$0.01 to \$1.42.

Experiment 2: $p = 0.95$.

In this experiment, the p value in the chance constraint (2) was increased to 0.95—a higher safety margin in order to deliver the superior travel condition for the HOT lane.

Figure 4-6 and Figure 4-7 present the results from one of the ten simulation replications (Exp. 2, Run 3). It was observed that the general trends of the inflows, the queue lengths, and the toll rates were similar to the results of Experiment 1. The toll rates (Figure 4-6) range from \$0.97 to \$1.50 when the demand was higher. The facility kept operating as an HOT lane for

only one additional time interval with a toll rate of \$0.24 after the upstream arrival rate dropped at minute 48. The inflow to HOT lane ranged from 45 to 62 vehicles per time interval with an average value of 52.57, when HOT facility was active. The average was slightly higher than the target inflow of 51 vehicles per time interval. The queue was present on the HOT lane during three-time intervals: 13, 16, and 17 (minute 24 to 26 and 30 to 34). No queue was present after interval 25 + 4 = 29 (minute 58). The percent time when the queue was present for or the HOT lane was $3/21 = 14.29\%$, much higher than the target value of 5%. The maximum HOT queue length was 5.

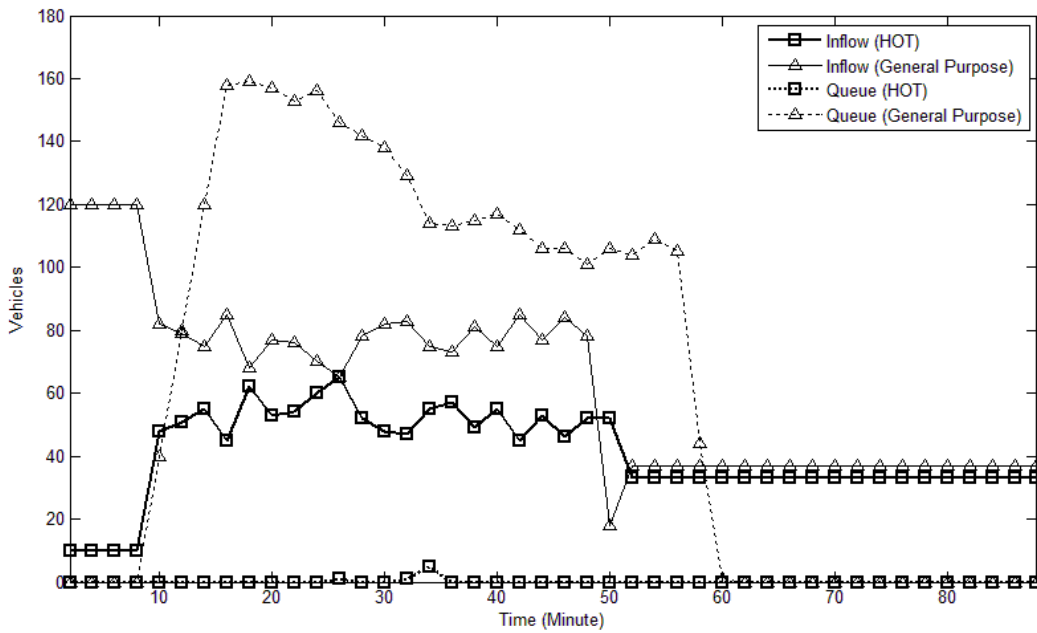


Figure 4-6. Facility performance (Exp. 2, Run 3).

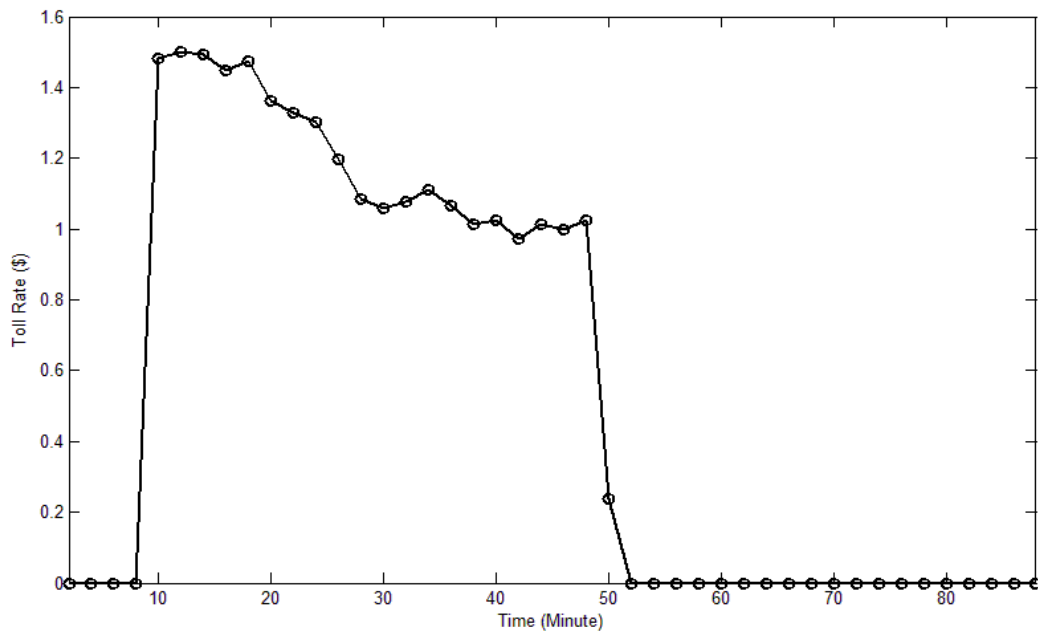


Figure 4-7. Toll rates (Exp. 2, Run 3)

Across the ten replications, the maximum queue length for the HOT lane varied from 0 to 5 vehicles, with an average value of 2.60. No queue was present beyond 4-time intervals after the last tolling interval. The average percentage time when the queue was present for the HOT lane was 6.43%, slightly higher than the operational goal of 5%. The toll rate ranged from \$0.06 to \$1.71.

CHAPTER 5 A TRADABLE CREDIT SCHEME FOR STAGGERED WORK TIME

INTRODUCTION

Traffic congestion is a direct result of the spatial and temporal concentration of travel demand. Historically, capacity expansion has been one of the primary solutions to the congestion problem. This approach turns out to be not viable, as it requires significant financial resource and right-of-way. More importantly, the added capacity would soon be consumed by induced travel demand (Duranton and Turner (2012)).

In contrast, travel demand management (TDM) strategies directly target travel demand and aim to spread it across space and time. Many TDM strategies have been proposed and some of them have been implemented in practice, e.g., congestion pricing (De Palma and Lindsey (2011), Tsekeris and Voss (2009)) and traffic rationing (Wang et al. (2010), Han et al. (2010)).

Alternative work schedules (Arnott et al. (2005), Mun and Yunekawa (2006)) are another TDM strategy that has been implemented to reduce traffic congestion. There are three types of alternative work schedules, i.e., staggered work hours where the firms assign different groups of travelers different work start times; flextime in which employees can adjust their arrival times, but need to be at workplace for some core times and fulfill the required working hours, and compressed work weeks in which employees work more hours per working days in order to compensate working for fewer days (Transportation Research Board (1980)).

Arnott et al. (2005) reported several real-world implementations of alternative work schedules in Manhattan in 1970, Toronto in 1970, Washington D.C. in 1970, Tel-Aviv in 1980, and Kuala Lumpur in 1998. He also remarked the voluntary staggered work plans of BMW and

Siemens in Germany as instances of involvement of firms in traffic congestion mitigation. In a four-week pilot program in Honolulu, Hawaii, the work hours of state, city, and county employees were changed from 7:45 AM–4:30 PM to 8:15 AM–5:15 PM. The subjected employees were 20% of 60,000 employees in downtown Honolulu. Although the program yielded reduction in average travel time, many employees did not like the mandatory shifting (Giuliano and Golob (1989)). Indeed, despite its considerable potential in mitigating traffic congestion, staggered work time has not been successful in practice due to the opposition of both employees and firms (Yoshimura and Okumura (2001)).

The observation that firms do not tend to participate in staggered work plans is explained by the theory of economic agglomeration, which suggests that the productivity of employees increases as the number of employees who work simultaneously increases. Staggering employees reduce the overlap of working hours and thus leads to some productivity loss. This explains why firms often do not voluntarily enroll in a staggered work schedule. However, firms' production technology may vary substantially. At some firms, employees complement each other and thus its productivity is largely compromised if employees do not work at the same time. At others, employees work more independently and their productivity is not affected too much if a portion of employees starts to work after the morning peak period. Such heterogeneity is utilized to design policies to encourage firms to stagger their employees to reduce traffic congestion. This chapter is one of such attempts.

More specifically, this chapter proposed a market-based mechanism to mitigate the negative consequence that firms may experience in staggering the work start time of their employees. In our proposed scheme, mobility credits were first allocated by a government agency to all firms in a central business district (CBD), and firms were responsible for

redistributing the credits to their employees. In addition, the credits are traded freely among firms. During the morning peak, each traveler who enters the CBD was charged one credit. Because the number of allocated credits to each firm was not enough to fulfill all the travel needs of their employees, each firm may eventually have two groups of employees: employees with credits who arrived during the charging interval, i.e. the morning peak, and employees without credits who shifted to another work start time.

The proposed scheme belongs to a category of tradable mobility credit schemes that recently have received considerable attention. The potential of tradable permits in regulating traffic congestion externality was first noted by Verhoff et al. (1997) and Viegas (2001). Recently, Yang and Wang (2011) proposed a mathematical framework for analyzing tradable mobility credits. Their work has been extended to capture the heterogeneity of travelers (Wang et al. (2012), Zhu et al. (2014)), transaction cost (Nie (2012)) and income effect (Wu et al. (2012)). Shirmohammadi et al. (2013) showed formally that there was a one-to-one correspondence between tradable credits and congestion pricing in idealized situations with perfect certainty. They further investigated a safety valve policy to balance regulation success and the volatility of credit price under demand and/or supply uncertainty. More recently, He et al. (2013) studied a tradable scheme when a finite number of Cournot-Nash (CN) players and an infinite number of Wardrop-equilibrium (WE) players compete in the network simultaneously. They analyzed how transaction costs would affect the trading and route-choice behaviors of both CN and WE players. For a more comprehensive review, see, e.g., Fan and Jiang (2013).

Our proposed scheme differed from those discussed above in that credits were allocated to eligible firms rather than individual travelers and trading in credits market were only allowed between firms instead of travelers. As such, the government agency needed only deal with a

limited number of players and subsequently the credit market was relatively smaller and easier to establish and monitor.

DESCRIPTION OF THE PROPOSED SCHEME

We described the proposed scheme in a simplified morning commute setting where all travelers who are traveling to the CBD every morning are employees of the firms in the CBD. The current common work start time is t^* and employees should be at workplace before t^* , i.e. no late arrival is allowed. To reduce congestion, a government agency decides the number of travelers who can enter the CBD during the morning peak, denoted by K , and issue K mobility credits. The mobility credits were allocated to firms, and firms were responsible for assigning them to their employees. During a charging period that starts from t^+ and ends on t^* , every traveler who wishes to enter the CBD was charged one mobility credit. Eventually, firm i with N_i employees had two groups of employees: \hat{N}_i employees with mobility credits, and \tilde{N}_i employees without credits. Clearly, only employees with credits could arrive during the charging interval. For employees without credits, firms could either change their work start time or require them to be at work place before t^+ . The latter option was less practical or desirable because it created much dissatisfaction among employees and caused a loss in productivity too. So, staggering work start time became a plausible option available to the firms. They shifted the work start time of employees without credits to \bar{t}^* , where $\bar{t}^* > t^*$. For simplicity, we further assumed that \bar{t}^* was the same for all firms and the duration between t^* and \bar{t}^* was long enough that all employees without credits would be able to enter the CBD before \bar{t}^* . More specifically, we assumed $\bar{t}^* - t^* = \frac{\sum_l \tilde{N}_l}{s}$, where s was the capacity of the highway leading to the CBD.

In the proposed scheme, mobility credits were not distributed directly among travelers and travelers were not allowed to trade their credits. Instead, mobility credits were initially endowed to the firms. Firms distributed them among their employees or traded them with other firms. Conceptually, firms with more complementary technology value more of having more employees at t^* and were likely a buyer in the credit market. On the other hand, firms with “independent” technology were less affected by staggering and would find themselves as a seller in the credit market.

Allocation of credits to firms rather travelers reduced the number of players in the market substantially. Hence, the market might be more tractable, and transaction costs associated with searching and negotiating with trading partners, monitoring the market and enforcement was reduced as well.

MODELING FRAMEWORK

This section introduced the modeling framework for analyzing the proposed scheme. Given the total number of credits issued by the government agency, K , we attempted to model firms’ decisions in the credit market and derived the equilibrium departure and arrival patterns of employees. Subsection “Impacts on travelers” mathematically described how the decisions of departure time of employees shape traffic demand pattern and presented the equilibrium cost of each group of employees based on the bottleneck model initialized by Vickrey (1969). Subsection “Impacts on firms” was devoted to the modeling of firms’ behaviors in the credit market. Subsection “Optimal design” formulated an optimal credit design problem based on the combination the equilibrium outcomes of firms and employees.

Impacts on Travelers

Morning commute problem

The morning commute problem was first introduced by Vickrey (1969) to describe the temporal distribution of morning commutes. Vickrey (1969) argued that, in addition to travel time, the deviation of actual arrival time from desired arrival time is an important factor in traveler's departure time decision. In fact, travelers who want to avoid traffic delay depart relatively early or late. On the other hand, travelers who arrive closer to the desired arrival time incur more travel delay. Smith (1984) and Daganzo (1985) proved, respectively, the existence and uniqueness of the equilibrium arrival pattern at a single bottleneck. For recent comprehensive reviews on the morning commute problem, see, e.g., Arnott et al. (1998) and de Palma and Fosgerau (2011).

Bottleneck model has been applied to investigate different tradable mobility credit schemes. Xiao et al. (2013) studied the efficiency of a tradable credits scheme with time-varying charging rate and showed a system optimum charging scheme can be designed for heterogeneous travelers if the distribution of the value of travel time is known. Nie (2012) proposed a tradable credit scheme that charges uniformly the travelers passing the bottleneck inside a peak time window and rewards mobility credits to travelers who travel outside of the peak time window. Nie and Yin (2013) further considered rewarding travelers who divert to alternative route or mode, in addition to those who travel during off-peak times.

In this chapter, we utilized the bottleneck model to derive the equilibrium travel cost of employees. To do so, the bottleneck model was briefly reviewed and then twisted to capture the specifications of our proposed scheme. Assume N homogenous individuals are commuting every

morning from their origin, i.e. home, to their workplaces located in the CBD. The capacity of the highway connecting the origin to the destination is s . Obviously, when $N \geq s$, not all travelers can arrive at workplace on time. Normalizing the free-flow travel time to zero and assuming no late arrival, the travel cost of a traveler who departs from home at time t is expressed as follows:

$$c(t) = \alpha T(t) + \beta \max\{0, t^* - t - T(t)\} \quad (1)$$

where $T(t)$ is the queuing delay; α is the value of travel time and β is the unit cost of arriving early to the destination, and $\alpha > \beta$. Therefore, each individual incurs a cost associated with being at the queue, referred as the delay cost, and a cost associated with not arriving on time, referred as the schedule cost. At equilibrium, the travel cost of all commuters would be the same and no commuter can reduce his or her travel cost by changing his or her departure time unilaterally. $T(t)$ is estimated by dividing the length of queue at the bottleneck at time t , i.e., $q(t)$, by the capacity of the bottleneck, i.e., s . At equilibrium, the last traveler must arrive at t^* ; otherwise he or she can save by arriving at t^* . The first departing traveler at t_s experiences no queuing delay; otherwise he or she can save by departing earlier. With a similar logic, it is inferred that the bottleneck should be fully utilized during the departing period $[t_s, t^*]$ and the departure rate from the bottleneck would be s . Thus $t_s = t^* - \frac{N}{s}$. Consequently, $q(t)$, which is the difference between the cumulative departure from home and the cumulative departure from the bottleneck can be written as:

$$q(t) = \int_{t_s}^t r(t)dt - s \cdot (t - t_s), t \in [t_s, t^*] \quad (2)$$

where $r(t)$ is the departure rate at time t . From the equilibrium definition of $\frac{\partial c}{\partial t} = 0$, (1) and (2) yield:

$$r(t) = \frac{\alpha}{\alpha - \beta} s, \quad t_s \leq t \leq t^*$$

It was straightforward to obtain the equilibrium travel cost as $\beta \frac{N}{s}$ and $q(t^*) = \frac{\beta}{\alpha} N$. The departure pattern before the implementation of the proposed scheme is depicted in Figure 5-1. In this situation, total travel cost and total travel delay are $\beta \frac{N^2}{s}$ and $0.5\beta \frac{N^2}{s}$ respectively.

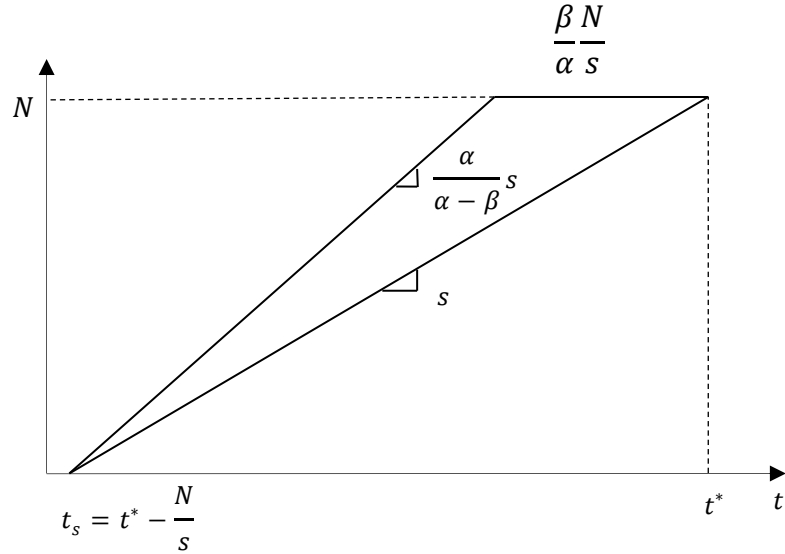


Figure 5-1. Departure pattern of employees before the implementation

Temporal Distribution Under The Proposed Scheme

Recall that under the proposed scheme, firms shifted the work start time of employees without credits to \bar{t}^* , where $\bar{t}^* > t^*$. As no late arrival was allowed, t^* and \bar{t}^* were set in a way that all employees without credits can arrive before \bar{t}^* . More specifically, it was assumed that $\bar{t}^* - t^* = \frac{\sum l \bar{N}_l}{s}$. This assumption completely separated the departures of the two groups of employees so that the temporal distribution of each group was analyzed separately.

For the group with credits, the first employee departed from home at $\hat{t}_s = t^* - \frac{\sum_i \tilde{N}_i}{s}$, and the last employee departed at $\hat{t}_e = t^* - \frac{\beta \sum_i \tilde{N}_i}{\alpha s}$. The equilibrium travel cost was $\beta \frac{\sum_i \tilde{N}_i}{s}$ and the total travel cost and travel delays were $\beta \frac{(\sum_i \tilde{N}_i)^2}{s}$ and $0.5\beta \frac{(\sum_i \tilde{N}_i)^2}{s}$, respectively. Similarly, for the group without credits, the first employee departed from home at $\bar{t}_s = \bar{t}^* - \frac{\sum_i \tilde{N}_i}{s}$, and the last employee departed at $\bar{t}_e = t^* - \frac{\beta \sum_i \tilde{N}_i}{\alpha s}$. The equilibrium travel cost was $\beta \frac{\sum_i \tilde{N}_i}{s}$ and the total travel cost and travel delays were $\beta \frac{(\sum_i \tilde{N}_i)^2}{s}$ and $0.5\beta \frac{(\sum_i \tilde{N}_i)^2}{s}$, respectively. The equilibrium departure pattern associated with the proposed scheme is depicted in Figure 5-2.

Given the total number of credits issued, we compared total travel cost, total travel delay, and total schedule cost before and after the implementation of the proposed scheme. The comparison suggested that all these measures are reduced by $2 \left(\frac{K}{N} \right) \left(1 - \frac{K}{N} \right)$. The maximum possible reduction was 50%, which was achieved by issuing credits of the half of the total number of employees.

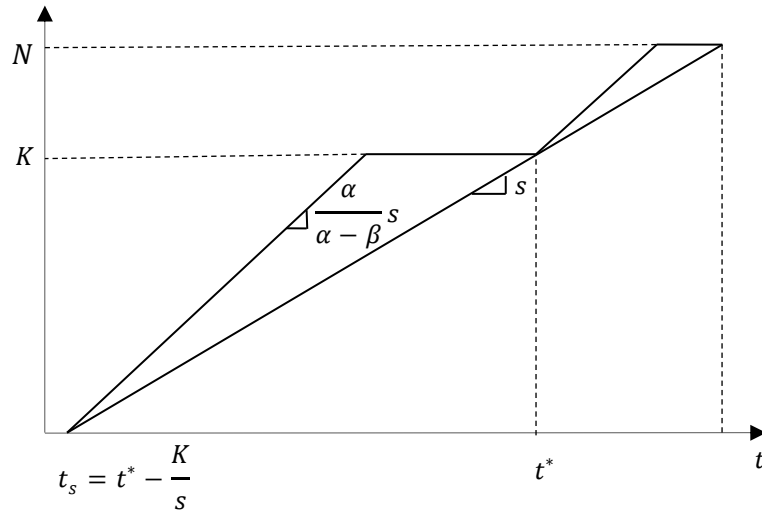


Figure 5-2. Departure pattern of employees under the proposed scheme

Impacts On Firms

Productivity Effect Of Work Start Time

It appeared that no empirical study has investigated the relationship between firm productivity and the work start time of its employees. Some researchers have suggested an indirect way to study the relationship (Yushimito et al. (2013)). Since a profit-maximizing firm determines its employees' wages to reflect their marginal productivity, investigating the variation of wages versus work start time may lead us to understand how productivity varies with the work start time. It should be emphasized that firm productivity can be affected by many factors, and establishing a function that addresses all these factors is challenging, if not impossible.

To our best knowledge, there were only two empirical studies that explored the relationship between wage and work start time. Wilson (1988) observed a strongly U-inverse relationship between them with the average wage of peak worker being twice of off-peak ones.

However, Arnott et al. (2005) argued that such a considerable difference in wage between peak and off-peak workers in Wilson's observation cannot "be explained by intraday productivity effect alone." He believed that such large differences stem from employees' abilities that were noticed by firms but "not observable to the empirical researcher."

In contrast to Wilson (1988), Gutiérrez-i-Puigarnau and Ommeren (2012) used panel data to have more control on a time-invariant characteristic of firms and workers, and found a slight inverse U-shaped relation between wage and work start time. Yushimito et al. (2013) explained the difference between Wilson (1988) and Gutiérrez-i-Puigarnau and Ommeren (2012) by referring to the time of these studies. With advancements in telecommunication technology, firms and employees can be in closer contact outside of workplace than they could at the time of the former study. Hence, the firms' productivity loss would be less, and wage is less sensitive to the work start time. Consistent with these earlier studies, Yushimito et al. (2013) defined the productivity obtained from a worker who arrives at time k as $\exp(\beta_0 + \beta_1 k + \beta_2 k^2)$, where, β_0 , β_1 , and β_2 are the parameters.

In this chapter, we assumed that the productivity of firm i contributed by $N_{i,j}$ employees with work start time t_j^* followed the following form:

$$\rho_{i,j}(N_{i,j}) = a_i e^{-\theta_i(t_j^* - t^*)^2} N_{i,j} \quad (3)$$

where a_i is the productivity of employees whose work start time is t^* , and θ_i is a parameter reflecting the sensitivity of firm's productivity to employees' work start time. A higher value of θ_i implied that firms were more affected by the deviation of work start time from t^* , while a lower value of θ_i was for less-sensitive firms. In other words, higher θ_i means firm's technology was complementary while lower θ_i suggests that employees were less dependent on each other.

The term of $e^{-\theta_i(t_j^*-t^*)^2}$ described the relative productivity of an employee in firm i with work start time t_j^* as compared to his or her co-worker who was assigned to initial work start time t^* .

It should be emphasized that Yushimito's productivity function is based on the arrival time to the workplace. In contrast, in Eq. (3) the productivity only depends on the work start time assigned to employees, not the actual arrival time to the workplace. Total productivity of firm i , denoted as ρ_i , was the sum of productivity resulted from all groups of employees, i.e.,

$$\rho_i = \sum_j a_i e^{-\theta_i(t_j^*-t^*)^2} N_{i,j} \quad (4)$$

According to (4), the productivity of firm i was maximized if all of its employees start to work on t^* , which corresponded to the situation without implementing the proposed scheme.

Firms' Behavior In The Credit Market

Under the proposed scheme, each firm should determine the number of credits needed. Firms were assumed to be profit maximizers and, therefore, each of them chose the number of credits to maximize its own profit. Here, the profit of firm i , π_i , is the total productivity minus the expense of purchasing credits from the market, i.e.,

$$\pi_i = a_i \widehat{N}_i + a_i e^{-\theta_i \left(\frac{\sum_l \widehat{N}_l}{s} \right)^2} \widetilde{N}_i - p(\widehat{N}_i - k_i^0) \quad (5)$$

Where p is the market price of credits and k_i^0 is the number of credits initially allocated to firm i . The first term in (5) is the total productivity resulted from employees with credits, who start to work at the primary work start time t^* , and therefore have no loss in their productivity. The second term in (5) is the total productivity resulted from employees without credits, who are shifted to the secondary work start time, \bar{t}^* , and the productivity resulted from each of them is

$a_i \cdot e^{-\theta_i(\bar{t}^* - t^*)^2}$ which is equal to $a_i \cdot e^{-\theta_i\left(\frac{\sum_l \tilde{N}_l}{s}\right)^2}$. Finally, the last term in (5) is the expense of purchasing extra mobility credits from the market. Note that when $\hat{N}_i < k_i^0$ the firm is a seller of credits and receive additional profit from selling extra credits; if $\hat{N}_i > k_i^0$, the firm is a buyer of credits and pays to purchase the extra mobility credits needed.

The decision that firm i faces can be expressed as a mathematical model as follows,

$$\max_{\hat{N}_i, \tilde{N}_i} \pi_i \equiv a_i \hat{N}_i + a_i e^{-\theta_i\left(\frac{\sum_l \tilde{N}_l}{s}\right)^2} \tilde{N}_i - p(\hat{N}_i - k_i^0)$$

s.t.

$$\hat{N}_i \geq 0 \tag{6}$$

$$\tilde{N}_i \geq 0 \tag{7}$$

$$\hat{N}_i + \tilde{N}_i = N_i \tag{8}$$

The decision variables of each firm, i.e. \hat{N}_i and \tilde{N}_i , not only have effect on the firm's profit, but also affect the profit of other firms. In addition, the market clearing condition can be written as,

$$0 \leq p \perp \sum_i k_i^0 - \sum_i \hat{N}_i \geq 0 \tag{9}$$

Equation (9) states that if the market is not cleared, i.e. there are more credits than needed, the price of credits would be zero.

The first-order optimality conditions for the above problem can be written as follows,

$$-a_i + p - \hat{\mu}_i + \xi_i = 0 \tag{10}$$

$$-a_i e^{-\theta_i \left(\frac{\sum_l \bar{N}_l}{s}\right)^2} \left[1 - \bar{N}_i \cdot \left(\frac{2\theta_i}{s}\right) \cdot \left(\frac{\sum_l \bar{N}_l}{s}\right) \right] - \bar{\mu}_i + \xi_i = 0 \quad (11)$$

$$0 \leq \hat{\mu}_i \perp \hat{N}_i \geq 0 \quad (12)$$

$$0 \leq \bar{\mu}_i \perp \tilde{N}_i \geq 0 \quad (13)$$

$$\hat{N}_i + \tilde{N}_i = N_i \quad (14)$$

where $\hat{\mu}_i$, $\bar{\mu}_i$, and ξ_i are the lagrangian multipliers associated with constraints (6), (7), and (8), respectively. At equilibrium, conditions (10)-(14) should be satisfied for each firm.

Assume that the credit market is cleared, and all firms staggered a positive number of employees, i.e., both \hat{N}_i and \tilde{N}_i are strictly positive. From (12) and (13) we have $\hat{\mu}_i = \bar{\mu}_i = 0$. In addition, by assuming a strictly positive of credit price, we have $\sum_i \hat{N}_i = \sum_i k_i^0 \equiv K$, and

$$\sum_i \tilde{N}_i = \sum_i N_i - K \quad (15)$$

From (10) $\xi_i = a_i - p$, and plugging this into (14) yields:

$$-a_i e^{-\theta_i \left(\frac{\sum_l N_l - K}{s}\right)^2} \left[1 - \tilde{N}_i \left(\frac{2\theta_i}{s}\right) \left(\frac{\sum_l \bar{N}_l}{s}\right) \right] + a_i - p = 0 \quad (16)$$

After some algebraic manipulation, we reach the following:

$$p = \frac{\sum_i \frac{1}{\theta_i} e^{\theta_i A^2} - \sum_i \frac{1}{\theta_i} + 2A^2}{\sum_i \frac{1}{\theta_i a_i} e^{\theta_i A^2}} \quad (17)$$

$$\tilde{N}_i = \frac{s}{2\theta_i A} \left[1 + \frac{p - a_i}{a_i} e^{\theta_i A^2} \right] \quad (18)$$

where $A = \frac{\sum_i N_i - K}{s}$. From (17), it was found that the credit price is independent of initial allocation of credits, which is consistent with Yushimito et al. (2013). In addition, \tilde{N}_i depends on the total number of employees, total issued credits, and productivity parameters of firm i , i.e. θ_i and a_i . That suggests that for a given total number of employees, changing the number of employees of a firm would not change its number of staggered employees. Such a property largely stems from the specification of the productivity function in which the productivity of each employee solely depends on his or her work start time, and would not be affected by the portion of employees who are shifted. In fact, given the total numbers of employees and issued credits, the total number of shifted employees are determined and firms based on their initial productivity and their sensitivity find their shares of shifted employees. Note that in deriving Eqs. (17) and (18), it is assumed that corner solutions do not exist, i.e. \tilde{N}_i and \hat{N}_i are strictly positives.

Optimal Design

As we discussed above, firms suffered by staggering their employees due to the projected loss of their productivity. The proposed scheme was able to compensate the firms to some extent. On the other hand, travelers were better off, because their travel cost was reduced by implementing the staggered work time. Therefore, one portion of players, i.e., firms, was worse off while the other portion, i.e., travelers, was better off. The goal of this section was to find an optimum number of credits to be issued by the government agency to maximize the social benefit, which was the total productivity of firms minus the total travel cost of employees, i.e.,

$$SB = \sum_i a_i (N_i - \tilde{N}_i) + \sum_i a_i e^{\theta_i \left(\frac{\sum_i N_i - K}{s} \right)^2} \tilde{N}_i - \beta \frac{K^2}{s} - \beta \frac{(\sum_i N_i - K)^2}{s} \quad (19)$$

where \tilde{N}_i was obtained from the previous Section. It was not difficult to verify from (19) that the social benefit only depends on K . Thus the maximization of social benefit, i.e.,

$\max_{0 \leq K \leq \sum_i N_i} SB(K)$, was a single-variable maximization problem. Unfortunately, a closed-form solution to the problem was not available. We used a numerical scheme to solve it instead.

NUMERICAL EXAMPLE

Suppose that there are two firms in the CBD, each with 1500 employees. The capacity of the bottleneck leading to the CBD was assumed to be 1000 *veh/hr*. Therefore, the peak period was three hours. For other parameters, $a_1 = a_2 = \$500/day$, $\beta = \$4/hr$. For each combination of θ_1 and θ_2 , the optimum number of K was obtained. Two scenarios were created based on the sensitivity parameter of firm 1. In the first case, $\theta_1 = 0.1$, which represents situations where firm 1 was a firm with moderately complementary employees. In the second case, $\theta_1 = 0.04$, representing a firm with less dependent employees. Figures 5-3 and 5-4 depict the number of shifted employees of each firm for the first and second scenario, respectively. It should be emphasized that the corner solutions are not activated for the ranges of θ_2 illustrated in Figures 5-3 and 5-4. It was observed in the second case, which represents less sensitivity to staggering, fewer mobility credits are issued by the government agency as compared to the first case. As expected, by increasing the sensitivity of firm 2, its shares in staggered employees were reduced.

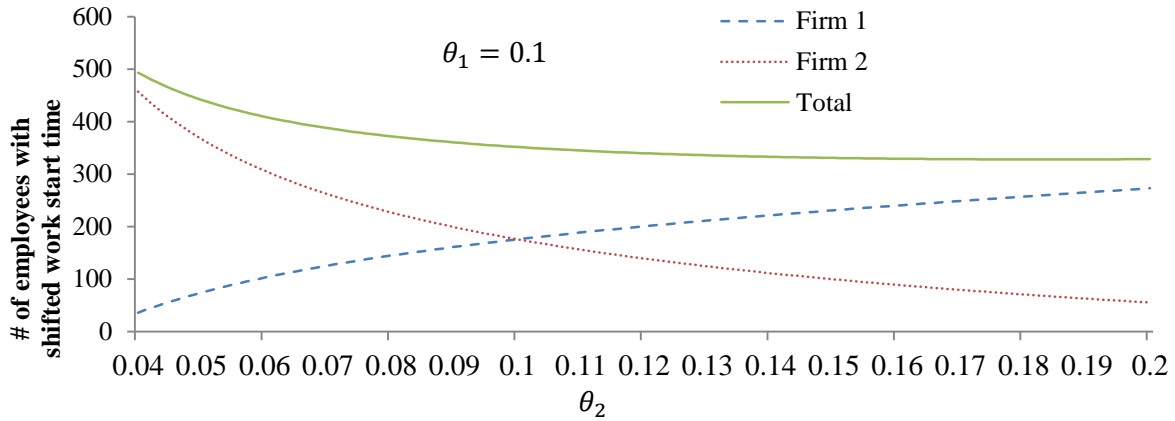


Figure 5-3. Number of shifted employees in scenario 1 ($\theta_1=0.1$)

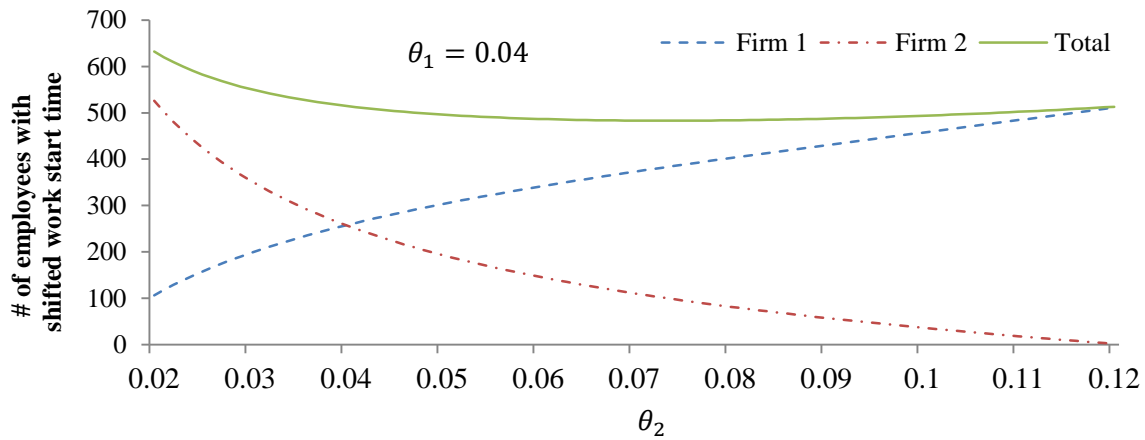


Figure 5-4. Number of shifted employees in scenario 2 ($\theta_1=0.04$)

Figure 5-5 shows the relation of credit price and a total number of employees. Among three combinations of low and moderate complementary technology, the lowest price was obtained when both firms have the low complementary technology. Surprisingly, the price of credits was lower when both firms had moderately complementary technology, compared to the case where firms have different levels of sensitivity. It was mainly because when both firms had

moderately complementary technologies, more credits were issued by the government agency at social optimum.

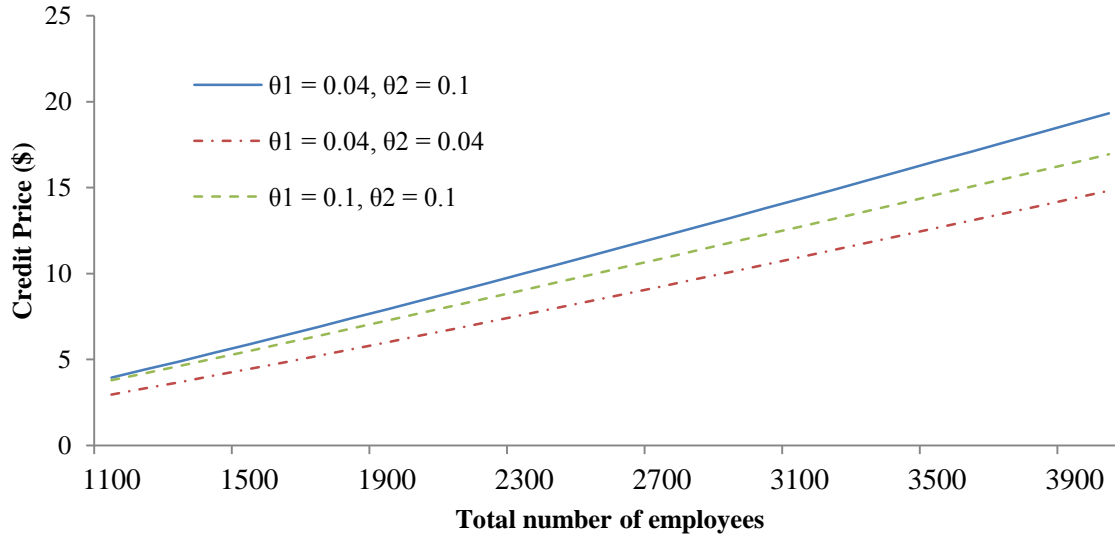


Figure 5-5. Variation of credit price

The social benefit was improved by the implementation of the proposed tradable credit scheme for all scenarios. Figure 5-6 shows that the improvement in social benefits increases as the bottleneck becomes more congested. As expected, when firms were less sensitive and traffic congestion was more severe, the social benefits improvement was more significant. However, firms were not necessarily better off. For an equal allocation of credits between two firms, both firms were worse off if firms had the same degree of sensitivity to staggering. However, when their degrees of sensitivity were different, the less sensitive firm would be better off as shown in Figure 5-7, while the firm with more complementary technology would be made worse off.

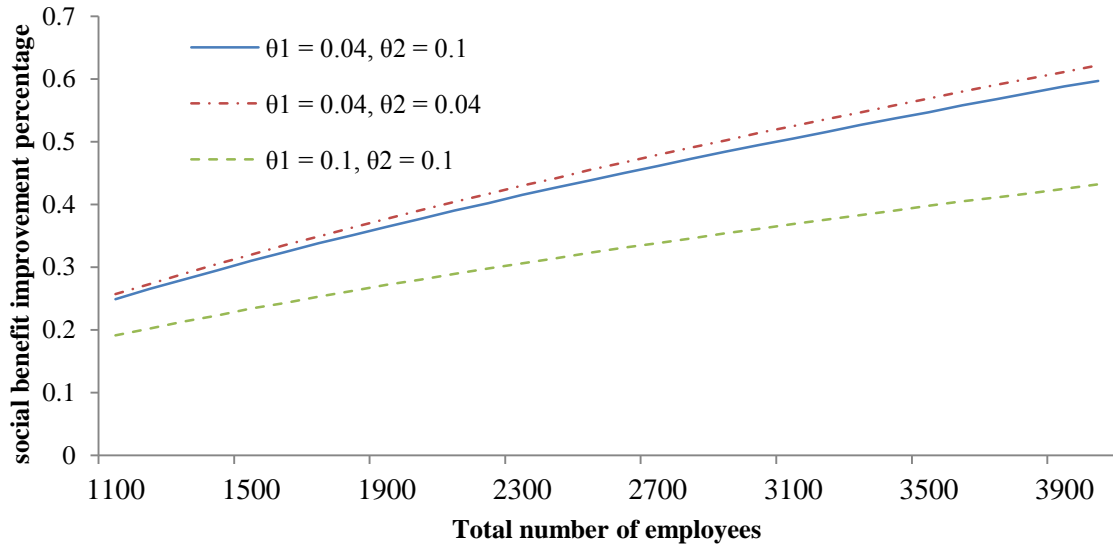


Figure 5-6. Social benefit percentage change compared to existing condition

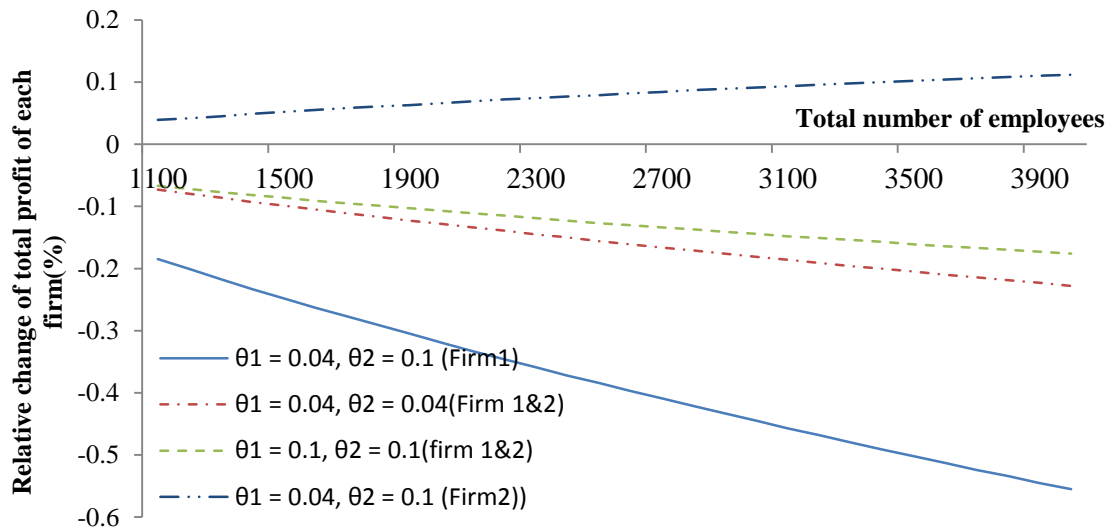


Figure 5-7. Relative change of total profit of firms

CHAPTER 6 CONCLUSIONS AND RECOMMENDATIONS

The questions that we answered in this research were: given the current state of the system, what is the toll that minimizes total system delay? What pricing strategy would produce the least total system delay? Is the linear toll pricing applicable to reality? Linear pricing strategies that were defined in Chapter 3 are intuitive to apply in practice and exhibit appealing properties. They allowed us to derive analytical expressions for all variables of interest for HOT lanes, including revenues and total delay in each alternative, which are linear functions of a single parameter, the pricing coefficient, a . How to determine this parameter depends on the operator (i.e. State Department of Transportation)'s objective, as outlined. From simulation experiments using *GTsim*, Variable Linear Toll strategy was selected as the most efficient pricing strategies to the perspective of the total delay, and the Fixed Toll strategy produced the largest revenue.

Approaches to determining optimal operational parameters for a proposed ML pricing scheme with refund option were proposed. Deterministic utility functions were adopted for each individual traveler with an underlying VOT distribution across the population. A modified point queue model for traffic propagation was developed to account for the intrinsic randomness in traffic flow. An optimization model with a chance constraint was established to determine the desired inflow to the HOT lane during each tolling interval. The relationship among the optimal operational parameters (including the toll rate, the refund amount, the premium for the refund option, the travel time saving guaranteed by the operator) was discussed for two operation paradigms. The preliminary results showed that models were able to capture important uncertainties in lane choices and traffic flow.

To alleviate the negative impact of staggered work schedules on firms, a tradable credit scheme was analyzed. The results of a numerical example showed that the proposed scheme can act as a relief for the productivity loss resulted from not having all employees at the desired work start times. Unfortunately, it did not necessarily provide an incentive for firms to stagger their employees. Although it could improve the social benefit, it was not a Pareto-improving scheme. The productivity function utilized to model the behaviors of firms under the proposed scheme did not reflect the effect of congestion cost on their productivity. However, there existed empirical evidence on the negative effect of traffic congestion on firms' productivity. If this effect of congestion is somehow reflected in the productivity function, then firms may also be made better off by the proposed scheme due to the congestion reduction. Eventually, their behaviors in the credit market would be to make a tradeoff between the negative impact of staggering employees and the positive impact from congestion mitigation. Future research should look in the situations that have more chance to find the proposed scheme Pareto improving that may function as an incentive mechanism to foster staggered work time.

REFERENCES

1. Supernak, J., Golob, J., Golob, T. F., Kaschade, C., Kazimi, C., Schreffler, E., and Steffey, D. (2002a). San diegos interstate 15 congestion pricing project: Attitudinal, behavioral, and institutional issues. *Transportation Research Record*, 1812, 78–86.
2. Supernak, J., Golob, J., Golob, T. F., Kaschade, C., Kazimi, C., Schreffler, E., and Steffey, D. (2002b). San diegos interstate 15 congestion pricing project: Traffic-related issues. *Transportation Research Record*, 1812, 43–52.
3. Supernak, J., Steffey, D., and Kaschade, C. (2003). Dynamic value pricing as instrument for better utilization of high-occupancy toll lanes. *Transportation Research Record*, 1839, 55–64.
4. Burris, M. W., and Stockton, B. R. (2004). Hot lanes in Houston-six years of experience. *Journal of Public Transportation*, 7 (3), 1–21.
5. Zhang, G., Yan, S., and Wang, Y. (2009). Simulation-based investigation on high occupancy toll lane operations for Washington state route 167. *Journal of Transportation Engineering*, 135 (10), 677–686.
6. Li, J. (2001). Explaining high-occupancy-toll lane use. *Transportation Research Part D*, 6 (1), 61–74.
7. Burris, M. W., and Appiah, J. (2004). Examination of Houstons quickride participants by frequency of quickride usage. *Transportation Research Record*, 1864, 22–30.
8. Podgorski, K. V., and Kockelman, K. M. (2006). Public perception of toll roads: A survey of the texas perspective. *Transportation Research Part A*, 40(10), 888–902.
9. Zmud, J., Bradley, M., Douma, F., and Simek, C. (2007). Attitudes and willingness to pay for tolled facilities: a panel survey evaluation. *Transportation Research Record*, 1996, 58–65.

10. Finkleman, J., Casello, J., and Fu, L. (2011). Empirical evidence from the greater Toronto area on the acceptability and impacts of hot lanes. *Transport Policy*, 18(6), 814–824.
11. Li, J., and Govind, S. (2002). An optimization model for assessing pricing strategies of managed lanes. No. 03-2082. *Proc., 82nd Annual Meeting of the Transportation Research Board*.
12. Zhang, G., Wang, Y., Wei, H., and Yi, P. (2008). A feedback-based dynamic tolling algorithm for high-occupancy toll lane operations. *Transportation Research Record*, 2065, 54–63.
13. Yin, Y., and Lou, Y. (2009). Dynamic tolling strategies for managed lanes. *Journal of Transportation Engineering*, 135(2), 45–52.
14. Lou, Y., Yin, Y., and Laval, J. A. (2011). Optimal dynamic pricing strategies for high-occupancy/toll lanes. *Transportation Research Part C*, 19(1), 64–74.
15. Laval, J., and Daganzo, C. (2006). Lane-changing in traffic streams. *Transportation Research Part B*, 40, 251–264.
16. Yin, Y., Washburn, S., Wu, D., Kulshrestha, A., Modi, V., Michalaka, D., and Lu, J. (2012). *Managed Lane Operations—Adjusted Time of Day Pricing vs. Near-Real Time Dynamic Pricing Volume I: Dynamic Pricing and Operations of Managed Lanes*. Final Report to Florida Department of Transportation.
17. Muñoz, J. C., and Laval, J. A. (2006). System optimum dynamic traffic assignment graphical solution method for a congested freeway and one destination. *Transportation Research Part B*, 40 (1), 1–15.

18. Laval, J. A. (2009). Graphical solution and continuum approximation for the single destination dynamic user equilibrium problem. *Transportation Research Part B*, 43 (1), 108–118.
19. Ungemah, D., Swisher, M., and Tighe, C. (2005). Discussing high-occupancy toll lanes with the denver, colorado, public. *Transportation Research Record: Journal of the Transportation Research Board*, (1932), 129-136.
20. Research and Innovative Technology Administration. (2014). Connected vehicle research in the United States. Retrieved January 25, 2014, from http://www.its.dot.gov/connected_vehicle/connected_vehicle_research.htm
21. Lou, Y. (2013). A unified framework of proactive self-learning dynamic pricing for high-occupancy/toll lanes. *Transportmetrica A-Transport Science*, 9(3), 205-222.
doi:10.1080/18128602.2011.559904
22. Gardner, L. M., Bar-Gera, H., and Boyles, S. (2013). Development and comparison of choice models and tolling schemes for high-occupancy/toll (HOT) facilities. *Transportation Research Part B*, 55, 142-153.
23. Duranton, G., and Turner, M. A. (2012). Urban growth and transportation. *The Review of Economic Studies*, 79(4), 1407-1440.
24. De Palma, A., and Lindsey, R. (2011). Traffic congestion pricing methodologies and technologies. *Transportation Research Part C*, 19(6): 1377–1399.
25. Tsekeris, T., and Voss, S. (2009). Design and evaluation of road pricing: state-of-the-art and methodological advances. *NETNOMICS: Economic Research and Electronic Networking*, 10, 5-52.

26. Wang, X., Yang, H., and Han, D. (2010). Traffic rationing and short-term and long-term equilibrium. *Transportation Research Record: Journal of the Transportation Research Board*, 2196(1), 131-141.
27. Han, D., Yang, H., and Wang, X. (2010). Efficiency of the plate-number-based traffic rationing in general networks. *Transportation Research Part E*, 46(6), 1095-1110
28. Arnott, R., Rave, T., and Schöb, R. (2005). Alleviating urban traffic congestion. *MIT Press Books*, 1.
29. Mun, S. I., and Yonekawa, M. (2006). Flextime, traffic congestion and urban productivity. *Journal of Transport Economics and Policy (JTPE)*, 40(3), 329-358.
30. Transportation Research Board (1980). *Alternative work schedules: Impacts on transportation*. Tech. Rep. NCHRP Synthesis of Highway Practice 73, Transportation Research Board, Washington, DC.
31. Giuliano, G., and Golob, T. F. (1989). *Evaluation of the 1988 Staggered Work Hours Demonstration Project in Honolulu: Final Report*. UCI-ITS-RR, 88-5, ISSN: 0193-5860;- UNTRACED, (88-5).
32. Yoshimura, M., and Okumura, M. (2001). Optimal Commuting and Work Start Time Distribution under Flexible Work Hours System on Motor Commuting. *Proceedings of the Eastern Asia Society for Transportation Studies*, 10(3), 455–69
33. Fan, W., and Jiang, X. (2013). Tradable mobility permits in roadway capacity allocation: Review and appraisal. *Transport Policy*, 30, 132-142.
34. Verhoef, E., Nijkamp, P., and Rietveld, P. (1997). Tradeable permits: their potential in the regulation of road transport externalities. *Environment and Planning B*, 24, 527-548.

35. Viegas, J. M. (2001). Making urban road pricing acceptable and effective: searching for quality and equity in urban mobility. *Transport Policy*, 8(4), 289-294.
36. Yang, H., and Wang, X. (2011). Managing network mobility with tradable credits. *Transportation Research Part B*, 45(3), 580-594.
37. Wang, X., Yang, H., Zhu, D., and Li, C. (2012). Tradable travel credits for congestion management with heterogeneous users. *Transportation Research Part E*, 48(2), 426-437.
38. Zhu, D. L., Yang, H., Li, C. M., and Wang, X. L. (2014). Properties of the multiclass traffic network equilibria under a tradable credit scheme. *Transportation Science (in press)*.
39. Nie, Y. M. (2012). Transaction costs and tradable mobility credits. *Transportation Research Part B*, 46(1), 189-203.
40. Wu, D., Yin, Y., Lawphongpanich, S., and Yang, H. (2012). Design of more equitable congestion pricing and tradable credit schemes for multimodal transportation networks. *Transportation Research Part B*, 46(9), 1273-1287.
41. Shirmohammadi, N., Zangui, M., Yin, Y. and Nie, Y. (2013). Analysis and design of tradable credit schemes under uncertainty. *Transportation Research Record*, 2333, 27-36.
42. He, F., Yin, Y., Shirmohammadi, N., and Nie, Y. M. (2013). Tradable credit schemes on networks with mixed equilibrium behaviors. *Transportation Research Part B*, 57, 47-65.
43. Vickrey, W. S. (1969). Congestion theory and transport investment. *The American Economic Review*, 59(2), 251-260.
44. Smith, M. J. (1984). The existence of a time-dependent equilibrium distribution of arrivals at a single bottleneck. *Transportation science*, 18(4), 385-394.
45. Daganzo, C. F. (1985). The uniqueness of a time-dependent equilibrium distribution of arrivals at a single bottleneck. *Transportation science*, 19(1), 29-37.

46. Arnott R, de Palma, A. and Lindsey, R. (1998). Recent developments in the bottleneck model. In: Button, K.J., Verhoef, E.T. (Eds.), *Road Pricing. Traffic congestion and the Environment: Issues of Efficiency and Social Feasibility*. Aldershot, Edward Elgar, UK, 161-179.
47. de Palma, A. and Fosgerau, M. (2011). Dynamic traffic modeling. In: de Palma, A., Lindsey, R., Quinet, E., Vickeman, R. (Eds.), *Handbook in Transport Economics*. Cheltenham, Edward Elgar, UK, 29-37.
48. Xiao, F., Qian, Z. S., and Zhang, H. M. (2013). Managing bottleneck congestion with tradable credits. *Transportation Research Part B*, 56, 1-14.
49. Nie, Y. M. (2012). A New tradable credit scheme for the morning commute problem. *Networks and Spatial Economics*, 1-23.
50. Nie, Y. M., and Yin, Y. (2013). Managing rush hour travel choices with tradable credit scheme. *Transportation Research Part B*, 50, 1-19.
51. Yushimito, W. F., Ban, X., and Holguín-Veras, J. (2013). Correcting the market failure in work trips with work rescheduling: an analysis using bi-level models for the firm-workers Interplay. *Networks and Spatial Economics*, 1-33.
52. Wilson, P. W. (1988). Wage variation resulting from staggered work hours. *Journal of Urban Economics*, 24(1), 9-26.
53. Gutiérrez-i-Puigarnau, E., and Van Ommeren, J. N. (2012). Start Time and Worker Compensation Implications for Staggered-Hours Programmes. *Journal of Transport Economics and Policy (JTEP)*, 46(2), 205-220.